

1 **Interacting Regime Shifts in Ecosystems: Implication for Early Warnings**

2 W.A. Brock<sup>1</sup> and S.R. Carpenter<sup>2,3</sup>

3  
4 A Manuscript for the 'Concepts and Synthesis' section of *Ecological Monographs*

5 31 December 2009

6  
7 <sup>1</sup>Department of Economics  
8 University of Wisconsin  
9 Madison, Wisconsin 53706

10  
11 <sup>2</sup>Center for Limnology  
12 University of Wisconsin  
13 Madison, Wisconsin 53706

14  
15 <sup>3</sup>corresponding author. email: srcarpen@wisc.edu

16

17 *Abstract.* Big ecological changes often involve regime shifts in which a critical threshold is  
18 crossed. Thresholds are often difficult to measure and transgressions of thresholds come as  
19 surprises. If a critical threshold is approached gradually, however, there are early warnings of the  
20 impending regime shift. For example, in a one dimensional ecosystem dynamics, autocorrelation  
21 approaches 1 from below, variance and skewness increase, and variance spectra shift to lower  
22 frequencies. Here we focus on variance, an indicator easily computed from monitoring data.

23

24 There are two distinct sources of increased variance near a critical threshold. One is the  
25 amplification of small shocks that occurs as the square of the modulus of the leading eigenvalue  
26 (or leading pair of eigenvalues in the complex case) approaches one from below. This source,  
27 called squealing, is well-studied. The second source of variance, called flickering, is brief  
28 excursions between attractors. Flickering has rarely been analyzed in the literature. Analysis  
29 presented here accounts for both sources of variance.

30

31 Complex systems exhibit many kinds of critical transitions. Interacting regime shifts may  
32 muffle or magnify variance near critical thresholds. Whether muffling or magnification occurs,  
33 and the size of the effect, depends on the product of the feedback between the state variables  
34 times the correlation of these variables' responses to environmental shocks. If this product is  
35 positive, magnification of the variance will occur. If the product is negative, muffling or  
36 magnification can occur depending on the relative magnitudes of these and other effects.  
37 Therefore, monitoring programs should measure variates that have opposite responses to the  
38 critical transition, because variance of at least one of these should be magnified as the critical  
39 transition is approached.

40

41 Simulation studies using a lake food web model suggest that muffling may sometimes  
42 interfere with detection of early warning signals of regime shifts. However, more important  
43 effects of muffling and magnification may come from their effect on flickering, when random  
44 shocks trigger a state change in a system with low resilience. Muffling decreases the likelihood  
45 that a random shock will trigger a regime shift. Magnification has the opposite effect.  
46 Magnification is most likely when feedbacks are positive and state variables have positively  
47 correlated responses to environmental shocks. These results help delimit the conditions when  
48 regime shifts are more likely to cascade through complex systems.

49

50 *Key words:* *Alternative stable states, critical transition, early warning flickering,, lakes, regime*  
51 *shift, squealing, trophic cascade, variance*

## INTRODUCTION

52  
53  
54 Scientists and managers are increasingly concerned with responses of complex systems to  
55 multiple interacting shocks. Massive shifts in energy, food and financial markets during 2007-  
56 2008 and their consequences for pollutant emissions and land use showed the connectedness of  
57 diverse sectors at the global scale. Linked global changes due to accelerating human activity are  
58 creating novel challenges for institutions concerned with managing climate, human health,  
59 ecosystem services and the economy (Walker et al. 2009). Connected regime shifts raise the  
60 possibility of cascading breakdowns in multiple services with consequences for human  
61 wellbeing.

62  
63 Some changes in complex systems are big, persistent, and difficult for managers to  
64 reverse (Holling 1973, Scheffer et al. 2001, Walker and Meyers 2004, Scheffer 2009). The  
65 generic term 'regime shift' represents this diverse class of big changes (Carpenter 2003, Scheffer  
66 and Carpenter 2003, Scheffer and Jeppesen 2007). In ecology, many different kinds of regime  
67 shifts are known from oceanic ecosystems, lakes, spatial dynamics of vegetation, drylands  
68 subject to desertification, rangelands subject to degradation, and others (Scheffer 2009).  
69 Mechanisms of ecological regime shifts are equally diversified. Examples include feedbacks  
70 between vegetation and the atmosphere (Foley et al. 2003, Narisma et al. 2007), soil (Rietkerk et  
71 al. 2004) or fire (Peters et al. 2004); biogeochemical feedbacks (Carpenter 2003); and complex  
72 interactions in food webs (Scheffer 1997, Jeppesen et al. 1998, Schmitz et al. 2006, Persson et al.  
73 2007).

74  
75 Regime shifts are hard to predict or anticipate (M.A. 2005). Gradual, incremental change  
76 may give the impression that an ecosystem is not capable of extensive change that goes beyond  
77 the range of historical experience (Carpenter 2002, 2003). Large and possibly unprecedented  
78 changes may occur, however, if the ecosystem crosses a critical threshold (Scheffer 2009). In a  
79 one-dimensional ecosystem model, a threshold is some point in state space such that crossing it  
80 leads to a shift from one attractor to another. Alternative stable states are a familiar ecological  
81 example. In a multi-dimensional dynamical ecosystem model, a threshold is an (n-1)-  
82 dimensional manifold embedded in the n-dimensional state space such that crossing this  
83 manifold leads to a shift in the dynamics from one attractor to another, where now an attractor  
84 can be a much more complicated object than a stable point.

85  
86 In empirical field studies and ecosystem management, thresholds for regime shifts are not  
87 known with precision. Also, thresholds may move over time, so estimates from one time interval  
88 may not apply to another time interval. When thresholds are estimated from finite datasets, their  
89 posterior probability distributions can be low and wide, with long tails (Carpenter 2003,  
90 Carpenter and Lathrop 2008). Such fat-tailed probability distributions for observed quantities  
91 may be common for important environmental parameters, with important implications for  
92 decisions and management (Weitzman 2009). Thus the difficulty of measuring ecosystem  
93 thresholds is important for applied as well as basic ecology.

94  
95 Recent studies show that some ecosystem variables change before regime shifts in ways  
96 that may serve as early warnings (Scheffer et al. 2009). These early warning signals may be  
97 useful even if the threshold is poorly known. For time series observations of ecosystem state

98 variables such as biomasses or chemical concentrations, standard deviations or variances may  
99 increase (Brock and Carpenter, 2006, Carpenter and Brock 2006, Brock et al. 2008), variance  
100 may shift to lower frequencies in the variance spectrum (Kleinen et al. 2003, Carpenter et al.  
101 2008, Biggs et al. 2009, Contamin and Ellison 2009), skewness may increase (Guttal and  
102 Jayaprakash 2008) and return rates in response to disturbance may decrease (van Nes and  
103 Scheffer 2007) in advance of a regime shift. If monitoring is in place to measure such signals,  
104 and managers are able to act swiftly to change key drivers, then catastrophic changes may  
105 sometimes be averted (Biggs et al. 2009, Contamin and Ellison 2009). The papers cited above  
106 establish the mathematical basis and simulation evidence for the indicators. Especially relevant  
107 for this paper, the appendix of Biggs et al. (2009) proves that the variance (or covariance matrix  
108 of a multidimensional system) becomes infinite (in a technical matrix sense) as the modulus of  
109 the leading eigenvalue moves from inside to outside the unit circle.

110  
111         So far, most theory for early warnings has considered situations in which an ecosystem is  
112 subject to a single kind of regime shift. Such systems gradually approach a critical transition as a  
113 driving variable changes slowly (Scheffer et al. 2009). But many interactions within ecosystems  
114 are capable of producing instabilities of various kinds (Ives and Carpenter 2007, Scheffer 2009).  
115 It is easy to imagine situations in which a given ecosystem is subject to multiple kinds of regime  
116 shifts. Moreover these regime shifts may be connected through other kinds of ecological  
117 interactions. If the individual regime shifts are connected ecologically, then proximity of one  
118 regime shift to its threshold may shift another regime shift toward or away from its threshold.

119  
120         This paper takes first steps toward understanding how interacting regime shifts may  
121 affect early warning signals. We focus here on variance. While a system may slow down even as  
122 it approaches a stable equilibrium, the approach to an unstable equilibrium must trigger a  
123 massive increase in variance (Biggs et al. 2009 Appendix). Moreover, variance is a familiar  
124 statistic that is easily measured using relatively short time series from a wide variety of  
125 ecosystems.

126  
127         The recent literature about rising variance near critical points is closely related to  
128 research on stochastic resonance (Wiesenfeld and Moss 1995). In multistable ecological systems  
129 driven by seasonal forcing, resonance can occur between the exogenous oscillating of the  
130 seasonal forcing and the endogenous potential oscillating of the dynamics themselves. If there is  
131 a slow moving parameter that drives the strength of the endogenous oscillations then there could  
132 be a bifurcation value of that parameter such that a small seasonal forcing could cause big  
133 oscillations of the dynamics as the parameter approaches its critical value. For example, Dushoff  
134 et al. (2004) discuss stochastic resonance in epidemiology and Schaffer et al. (2001) consider  
135 related ideas in predator-prey systems. Because we focus on exogenous forcing processes that  
136 are not seasonal here, it is beyond the scope of this paper to investigate early warning signals  
137 based upon ideas like stochastic resonance.

138  
139         In the next section of the paper, we distinguish between two different processes that can  
140 add to variance near critical transition points: squealing, which is an amplification of variance as  
141 the critical point is approached, and flickering, which is transient excursions between alternate  
142 basins of attraction. Previous studies have addressed squealing alone, whereas we account for  
143 both squealing and flickering effects on variance. We then introduce an ecological example that

144 involves two different regime shifts in a trophic cascade. This example is used throughout the  
 145 paper to illustrate the effects on variance of interacting regime shifts, drawing on mathematical  
 146 results which are derived in the Appendix. Interacting regime shifts can decrease (muffle) or  
 147 increase (magnify) variance of state variable time series. We discuss the conditions that lead to  
 148 muffling or magnification, and conclude that these effects of interacting regime shifts have  
 149 important implications for early warning indicators.

## 150 SQUEALING AND FLICKERING

151  
 152  
 153 As a stochastic dynamic system approaches a critical transition, the variance increases  
 154 sharply (Brock and Carpenter 2006, Carpenter and Brock 2006 Appendix S2, Brock et al. 2008,  
 155 Biggs et al. 2009 Appendix). Mathematically, this amplification of variance occurs because the  
 156 variance of the state variables is inversely proportional to the return rate of the system, and the  
 157 return rate approaches zero at the critical point (Carpenter and Brock 2006 Appendix S2, Biggs  
 158 et al. 2009 Appendix). This mechanism of variance amplification, which is well-studied in the  
 159 literature, is called squealing. Here we draw a distinction between squealing and another  
 160 mechanism of variance increase, called flickering. Flickering is caused by transient excursions  
 161 between two basins of attraction when the system is near a critical point.

162  
 163 To understand the distinction consider a discrete-time system with two alternative stable  
 164 points separated by an unstable point (Fig. 1). The solid curve in each panel connects the state  
 165 variable value at time  $t$  ( $x_t$ ) with its value at the next time step ( $x_{t+1}$ ). The dotted diagonal line  
 166 shows equilibria, i.e.  $x_t = x_{t+1}$ . Many textbooks show how discrete-time systems can be analyzed  
 167 using diagrams of  $x_t$  versus  $x_{t+1}$  (May and McLean 2007). The gray curves show the range of  $x_{t+1}$   
 168 that can occur after any specified value of  $x_t$  due to random variation. For this example, we  
 169 assume that no values can occur outside of the upper and lower gray curves.

170  
 171 Fig. 1A shows the base case of two stable points separated by an unstable point. The  
 172 other panels show outcomes when the curve is gradually raised so that the lower equilibrium  
 173 becomes less stable. Two different sources of variance increase as the curve of Fig. 1A rises with  
 174 respect to the diagonal line. First, variance may increase as the slope of the solid black curve at  
 175 the intersection with the dashed line approaches one from below (Fig. 1B) (Carpenter and Brock  
 176 2006, Biggs et al. 2009). This source of increased variance is squealing. Second, variance may  
 177 increase because of brief excursions from one attractor to the other (Fig. 1C). In Fig. 1C, starting  
 178 at the low equilibrium, a large shock can move the system past the unstable equilibrium into the  
 179 basin of attraction of the upper equilibrium. This kind of variance, which we call “flickering”,  
 180 can occur only if the stochastic envelope around the curve includes all three equilibria.  
 181 Flickering may increase variance over many time steps if the system moves back and forth  
 182 between the stable attractors over a period of time. In the Appendix, we make the notion of  
 183 flickering more precise and establish a framework to study squealing and flickering in systems  
 184 where multiple critical transitions can interact. Finally, the curve may rise so far that the lower  
 185 equilibrium no longer exists (Fig. 1D). In this case, the system has passed through the critical  
 186 transition and only one stable equilibrium exists.

187  
 188 To emphasize the distinction between squealing and flickering we introduce an example  
 189 that can flicker but not squeal (Fig. 2). The map from  $x_t$  to  $x_{t+1}$  is a straight solid black line with a

190 discontinuity at  $x_t = 2$ . This is a special case of the system studied by Peterson et al. 2003. As in  
 191 Fig. 1 the equilibria occur where the solid black line crosses the dashed line, and the gray lines  
 192 denote the upper and lower bounds of random variability. The model can have two alternative  
 193 stable states and an intermediate unstable state. As the solid black lines move upward, there is a  
 194 critical transition where the lower equilibrium disappears. Squealing is not possible because the  
 195 slope of the black line is constant. However, flickering can occur near the critical point as the  
 196 system jumps between the two equilibria. Indeed, flickering can occur even if the slope of the  
 197 solid black lines is zero (Fig. 2B).

#### 199 MULTIPLE TRANSITIONS IN TROPHIC CASCADES

200  
 201 Even though ecosystems are subject to many kinds of critical transitions (Scheffer 2009),  
 202 most (though not all) studies of critical transitions in ecology have attempted to isolate one  
 203 particular transition for analysis. Perhaps this is because field study of critical transitions is quite  
 204 difficult in ecology, so it is simpler to focus on one transition at a time (Carpenter 2003, Scheffer  
 205 and Carpenter 2003, Petraitis and Latham 1999). Yet it is likely that any given ecosystem could  
 206 potentially undergo many distinct critical transitions. If two different critical transitions are  
 207 linked in some way, then observed time series of system behavior could bear the signature of  
 208 both transitions.

209  
 210 As a specific example, we address cascading changes in lake ecosystems, which are well-  
 211 studied in the context of critical transitions (Carpenter 2003, Carpenter et al. 2008, Scheffer et al.  
 212 2000). A large body of field studies and models suggest that big changes in food webs of lakes  
 213 may involve more than one critical transition. Several examples involve interactions of benthic  
 214 and open-water subsystems, or littoral and pelagic sub-systems (Scheffer 2009). Here we  
 215 consider two distinct but linked critical transitions that involve fish and zooplankton (Fig. 3)

216  
 217 Theory and experiments show that massive shifts in fish populations cascade to  
 218 phytoplankton, thereby changing primary production and a host of associated ecosystem  
 219 processes (Carpenter and Kitchell 1993). Such big changes in the fish community can result from  
 220 a trophic triangle (Ursin 1982) involving adults and juveniles of the apex predator interacting  
 221 with smaller-bodied species of fish.

222  
 223 A trophic triangle involving largemouth bass and golden shiners is embedded in Fig. 3  
 224 (gray boxes). This triangle is dominated by the apex predator if adult biomass is large enough to  
 225 suppress populations of the smaller-bodied fish species, or by the smaller-bodied fishes if  
 226 mortality is high for adult apex predators. High mortality can be inflicted by fishing, resulting in  
 227 a type of alternative state called “compensation-depensation” by Walters and Kitchell (2001).  
 228 Theory suggests that (1) plausible models for the fish shift can be represented as a critical  
 229 transition, (2) various time-series statistics such as autoregression coefficients, variance and its  
 230 multivariate analogs, skewness and variance power spectra change in predictable ways prior to  
 231 the critical transition, and (3) these statistical signals are transmitted downward through the food  
 232 chain to zooplankton and phytoplankton (Carpenter et al. 2008).

233  
 234 A second type of critical transition can occur in the plankton (Fig. 3, hatched boxes). The  
 235 trophic interactions among carnivorous invertebrates such as the phantom midge (*Chaoborus*),

236 large-bodied herbivorous crustaceans such as *Daphnia*, and small-bodied herbivorous  
 237 crustaceans such as *Bosmina* or small diaptomid copepods can produce sharp transitions in  
 238 grazer body size, community composition, morphology and behavior (Dodson 1974, Neill 1975,  
 239 Hall et al. 1976, Kerfoot 1980). If planktivory by fishes is low, mortality of phantom midges and  
 240 large-bodied *Daphnia* is low. While small *Daphnia* can be consumed by phantom midges, large-  
 241 bodied *Daphnia* have life-history and morphology adaptations that enable them to reach high  
 242 abundance even when phantom midges are abundant (Hall et al. 1976, Kerfoot 1980). Small-  
 243 bodied grazers are, however, vulnerable to phantom midges and can be suppressed by phantom  
 244 midge predation. If phantom midge abundance is reduced by fish predation, small-bodied grazers  
 245 become dominant. Thus, as planktivory by fishes is adjusted upward or downward there are  
 246 strong shifts in body size of herbivorous crustaceans, mediated by phantom midge or other  
 247 carnivorous invertebrates. These shifts appear to be alternative stable states (Neill 1988). They  
 248 are linked to, but distinct from, the critical transitions studied in piscivore-planktivore systems.  
 249

250         What happens if the critical points for these transitions occur close together in time? This  
 251 is not just a matter of chance. Connected transitions in multi-dimensional systems occur when  
 252 critical manifolds are crossed, and the intersections of manifolds have fewer dimensions than the  
 253 manifolds themselves. Discontinuities occur in the transition to the low-dimensional  
 254 intersections. In time series observations, one could imagine several different possibilities. The  
 255 statistical signals of the different transitions might fall in sequence, leading to a cascade of  
 256 increasingly intense signals. Or the statistical signals may blur together, perhaps obscuring any  
 257 early warning signal. This is the general issue that we wish to explore.  
 258

#### 259                   INTERACTING REGIME SHIFTS: MUFFLING OR MAGNIFYING VARIANCE

260  
 261         As a gradual change in a driving variable moves a one-dimensional system toward a  
 262 critical threshold (e.g. the upward movement of the solid black lines in Fig. 1), the approach to  
 263 the threshold will be announced by growing variance caused by squealing and flickering. Will  
 264 the same early warnings occur in a more complex system with multiple thresholds? The answer  
 265 is not obvious. Interactions in the more complex system could muffle or magnify variance.  
 266

267         To make this question more precise, we compare the variance of a state variable  
 268 approaching a threshold in isolation to the variance that occurs when the same critical transition  
 269 is embedded in a more complex system. For a given state variable, we define muffling and  
 270 magnifying in terms of two variances: the variance of the state variable as if it existed alone in  
 271 isolation from the rest of the system, versus the variance of the state variable when it is part of  
 272 the interacting system. If the variance of the state variable in isolation is greater than the variance  
 273 when the state variable is embedded in the system, then the larger system *muffled* the variance.  
 274 Conversely, if the variance in isolation is smaller than the variance when the state variable is  
 275 embedded in the system, then the larger system *magnified* the variance.  
 276

277         The concepts of muffling and magnifying are made precise mathematically in the  
 278 Appendix. There we derive conditions for muffling or magnifying in a rather general model of  
 279 two interacting state variables, each subject to a critical transition. These conditions account for  
 280 both squealing and flickering. Flickering is important because a brief excursion between  
 281 attractors in one state variable could trigger changes in the other state variable. Below we present

282 an ecological example to illustrate muffling and magnifying. The example is a special case of the  
 283 more general results presented in the Appendix.

#### 284 AN ECOSYSTEM EXAMPLE

285  
 286  
 287 We now turn to a model of a lake ecosystem subject to two different but coupled critical  
 288 transitions: compensation-dependence in the fish community and the shift between large-bodied  
 289 and small-bodied herbivorous crustaceans in the zooplankton (Fig. 3). We consider gradual  
 290 increase in fishing of the piscivore as the exogenous slow driver (Carpenter et al. 2008).  
 291 Increasing fishing mortality of adult piscivores will eventually release the planktivores to surge  
 292 in biomass as they cross a critical transition. At some level of planktivory by fishes, large-bodied  
 293 zooplankton will suffer high planktivory and collapse in biomass to be replaced by small-bodied  
 294 zooplankton. But it is not at all clear whether the threshold for the zooplankton shift occurs  
 295 before, at the same time, or after the threshold for the planktivorous fishes. Here we abstract the  
 296 complex interactions of Fig. 3 and consider only the planktivorous fishes and large-bodied  
 297 herbivorous crustacean zooplankton as indicator variables for the two critical transitions. The  
 298 fish dynamics are assumed to provide the slower-moving driver for the plankton dynamics. We  
 299 ask how the dynamics are affected by variance due to the two critical transitions that can occur in  
 300 the system.

#### 301 302 *Variance When Two Thresholds Interact*

303  
 304 Methods presented in the Appendix are used here to derive an amplification index that is  
 305 proportional to the degree of muffling or magnifying conferred by a system. The equation for the  
 306 amplification index reveals some general features of systems that tend to muffle or magnify  
 307 variance. The model is

$$308 \quad (1) \quad x_{i,t+1} = x_{it} \exp[f_i(x) + b_{ii}e_{i,t+1}], \quad i=1,2.$$

309  
 310 The  $x_i$  are the state variables, each of which changes over time according to a rate function  $f_i(x)$   
 311 that depends on both state variables (Table 1). Each state variable is subject to small exogenous  
 312 environmental shocks  $e_i$ , where  $\{e_i\}$  is a stationary sequence of random variables, each with mean  
 313 zero and fixed standard deviation. The shocks to the state variables are uncorrelated over time,  
 314 but may be correlated between state variables at each time step. The parameters  $b_{ii}$  determine the  
 315 effect of the shocks on the dynamics.

316  
 317 To evaluate the variance of the system, we first linearize the model around an equilibrium  
 318 that is gradually destabilized by slow increase in fishing mortality of the piscivore (Carpenter et  
 319 al. 2008). The linearization around steady states is a special case of the model analyzed in the  
 320 Appendix. Let  $\bar{x}_i, i = 1, 2$  denote the components of a positive deterministic steady vector of  
 321 equation (1) when the  $e$ 's are set equal to zero, i.e.  $f_i(\bar{x}_1, \bar{x}_2) = 0, i=1,2$ .

322  
 323 Let  $y_{it} := x_{it} - \bar{x}_i, i=1,2$ , where the notation ':= ' means 'is defined to be'. Define  
 324  
 325  $f_{y_i} := \frac{df_i(y_i)}{dx}$ , and expand the system (1) in a Taylor series around the 2x1 vector  $\bar{x}$  to obtain

326

$$327 \quad (2a) \quad y_{1,t+1} = (1 + \bar{x}_1 f_{1x_1}) y_{1t} + \bar{x}_1 f_{1x_2} y_{2t} + \bar{x}_1 b_{11} e_{1,t+1} + o(y_t, b_{11} e_{1,t+1})$$

328

$$329 \quad (2b) \quad y_{2,t+1} = \bar{x}_2 f_{2x_1} y_{1t} + (1 + \bar{x}_2 f_{2x_2}) y_{2t} + \bar{x}_2 b_{22} e_{2,t+1} + o(y_t, b_{22} e_{2,t+1})$$

330

331 where  $o(y_t, b_{ii} e_{i,t+1})$ ,  $i=1,2$  are functions that go to zero faster than the norm of  $y_t$  plus the  
 332 absolute value of  $b_{ii} e_{i,t+1}$   $i=1,2$  go to zero. Hence the shocks as well as the deviations must be  
 333 small in order for the linear part of equation (2) to be a good approximation. Furthermore we  
 334 assume both eigenvalues of the linearization matrix in equation (2) are inside the unit circle of  
 335 the complex plane. This assumption implies that the steady state vector  $\bar{x}$  is locally  
 336 asymptotically stable and that the matrix equation (4) below has a unique solution (Biggs et al.  
 337 (2009, Appendix)).

338

339 We write the linear part of (2) in matrix form as

340

$$341 \quad (3) \quad y_{t+1} = \rho y_t + n_{t+1},$$

342

343 where the elements of the matrix  $\rho$  and the vector  $n$  come from (2). Equation (3) corresponds to  
 344 Appendix equation (5c) where the 2x1 vector  $y_{t+1} = x_{t+1}$ , the 2x1 vector  $\bar{a}$  is the 2x1 zero  
 345 vector, the 2x2 matrix  $\rho$  is the 2x2 matrix of linearization terms multiplying the  $y$ 's in (2), the  
 346 2x2 matrix  $b$  is a 2x2 diagonal matrix with diagonal terms multiplying the  $e$ 's in (2), the matrix  
 347  $\beta$  is the matrix of all zeroes,  $S_2(x_{3t}) = 0$ , and the 2x1 vector  $f_t$  is the 2x1 zero vector. We  
 348 analyze the triangular case where  $\rho_{21} = 0$ . This corresponds to the lake trophic cascade example  
 349 where the fishes switch to other prey when large-bodied zooplankton are scarce.

350

351 The steady-state moment matrix (following equation 7C of the Appendix) is

352

$$353 \quad (4) \quad E_{\infty} y_t y_t' = \rho E_{\infty} y_t y_t' \rho' + \Sigma_n$$

354

355 where  $n_{i,t+1} := b_{i1} e_{1,t+1} + b_{i2} e_{2,t+1}$ ,  $i=1,2$ , and  $\Sigma_n := E n_t n_t'$ . The shocks  $\{e_{ij}\}$  are assumed to be mean  
 356 zero second order stationary processes so, therefore, the impacts  $\{n_{ij}\}$  are also second order  
 357 stationary processes. Although these impacts  $\{n_{ij}\}$  are uncorrelated over time, these impacts to  
 358 the state variables can be contemporaneously correlated with correlation coefficient  
 359  $r_{n,12} := \Sigma_{n,12} / (\Sigma_{n,1,1}^{0.5} \Sigma_{n,2,2}^{0.5})$ . We drop the subscript  $n$  on the correlation coefficient and  $\Sigma$  to ease  
 360 notation where the connection to  $n$  is clear from context.

361

362 Recall that symmetry of the steady state moment matrix  $M := E_{\infty} y_t y_t'$  implies (4) is just a  
 363 system of three equations in three unknowns,  $M_{11}, M_{12} = M_{21}, M_{22}$ . Hence the system (4) may be  
 364 expressed as a linear system of three equations and three unknowns. When the off diagonal terms  
 365  $f_{ix_j}, i \neq j$  are set equal to zero, we have

366

367 (5)  $M_{ii,diag} = \Sigma_{n,ii} / (1 - \rho_{ii}^2)$ .

368

369 Here  $\Sigma_{n,ii}$  denotes the (i,i) element of the 2x2 moment matrix  $\Sigma_n$  which was defined above.

370

371 It is clear from (5) that if the system is diagonal and there is a slow variable that is  
 372 gradually pushing  $\rho_{ii}^2$  up to one from below then the steady state variance  $M_{ii,diag}$  goes to  
 373 infinity. This is an early warning signal of a bifurcation where an eigenvalue of a linearization  
 374 passes through +1. We are interested in locating sufficient conditions on  $\rho, n$  such that muffling  
 375 (magnifying) occur,

376

377 (6)  $M_{ii} < M_{ii,diag}, (M_{ii} > M_{ii,diag})$

378

379 We may write a system of three linear equations in the three unknowns  $M_{11}, M_{12} = M_{21}, M_{22}$   
 380 from (4) and solve it using Cramer's Rule or, equivalently by using the inverse of the associated  
 381 3x3 matrix of weights on the three M's from (4). An alternative approach using Kronecker  
 382 products is discussed by Ives et al. (2003). Here we apply Cramer's rule to solve for  $M_{11}$  and  
 383 obtain the condition (7) for the "triangular" case where  $\rho_{21} = 0$ ,

384

385 (7) 
$$\begin{aligned} \text{muffling } & \rho_{12}^2 \Sigma_{n22} + 2\rho_{12}\rho_{11}[r_{12}\Sigma_{n,11}^{1/2}\Sigma_{n,22}^{1/2}(1 - \rho_{22}^2) + \Sigma_{n,22}\rho_{12}\rho_{22}] / (1 - \rho_{22}\rho_{11}) < 0 \\ \text{magnifying } & \rho_{12}^2 \Sigma_{n22} + 2\rho_{12}\rho_{11}[r_{12}\Sigma_{n,11}^{1/2}\Sigma_{n,22}^{1/2}(1 - \rho_{22}^2) + \Sigma_{n,22}\rho_{12}\rho_{22}] / (1 - \rho_{22}\rho_{11}) > 0 \end{aligned}$$

386

387 The left side of (7) is an amplification index. It tells us whether variance is decreased or  
 388 increased by the full set of interactions. If  $r_{12}$  and  $\rho_{12}$  are the same sign, then the amplification  
 389 index must be positive and variance must be magnified by the interactions. If  $r_{12}$  and  $\rho_{12}$  are  
 390 opposite in sign, then the amplification index could be negative if the first term and last term of  
 391 the amplification index are sufficiently small. If the amplification index is negative then the  
 392 variance is decreased by the interaction. To see why the outcome depends on the signs of  $r_{12}$  and  
 393  $\rho_{12}$ , remember that the diagonal  $\rho$  terms are less than unit magnitude and positive. Therefore the  
 394 amplification index must be positive if  $r_{12}\rho_{12}$  is positive. If  $r_{12}\rho_{12}$  is negative, then the second  
 395 term of the amplification index is negative and if it is sufficiently large in magnitude then the  
 396 amplification index will be negative.

397

### 398 *Threshold Interactions in a Simulated Food Web*

399

400 We simulated the dynamics of planktivorous fish ( $x_2$ ) and large-bodied zooplankton  
 401 grazers ( $x_1$ ) using

402

403 (8) 
$$\begin{aligned} x_{i,t+1} &= x_{i,t} e^{f(x_i)} \\ f(x_{i,t}) &= -c_i(x_{i,t} - a_{l,i})(x_{i,t} - a_{c,i})(x_{i,t} - a_{u,i}) + s_{i,t} + N_{i,t} \end{aligned}$$

404

405 Equilibria are the  $a$ 's with subscripts denoting the lower stable root ( $l$ ), intermediate unstable  
 406 root or critical transition point ( $c$ ), and upper stable root ( $u$ ) (Table 1). The parameter  $c_i$  scales the

407 per-time-step growth of state variable  $i$ . The noise  $N_{i,t}$  is independently and identically distributed  
 408 multivariate normal with mean zero and variance-covariance matrix  $\Sigma$ . This noise represents  
 409 exogenous random inputs such as variations in water temperature or other physical-chemical  
 410 drivers. Shocks to the state variables are correlated within each time step but uncorrelated across  
 411 time. The  $s_{i,t}$  are slowly-changing variables where  $s_2$  represents changes to the fish community  
 412 caused by slow changes in fishing mortality of an apex predator. The fish variable  $x_2$  changes  
 413 more slowly than the zooplankton variable  $x_1$ . Planktivore generation times are two or more  
 414 years, whereas zooplankton generation times are about one to three weeks. Therefore it is  
 415 plausible that  $x_2$  can act as a slow variable for the dynamics of  $x_1$ . The interaction is represented  
 416 by  $s_{1,t}$  which not a constant, but changes over time as a function of  $x_{2,t}$ . Specifically we assumed  
 417

$$418 \quad (9) \quad s_{1,t} = k\bar{x}_{2,t}$$

419  
 420 where  $\bar{x}_{2,t}$  is the lower stable equilibrium of planktivores given the current value of  $s_{2,t}$ . The  
 421 sign of  $k$  can be positive or negative depending on the zooplankton group represented by  $x_1$ .  
 422 Large-bodied herbivorous zooplankton have a negative relationship to  $x_2$ , whereas small-bodied  
 423 herbivorous zooplankton have a positive relationship to  $x_2$ .  
 424

425 Simulation studies examined muffling or magnification of variance for both negative and  
 426 positive values of  $k$  (Fig. 4). In each case, we compared four sets of simulations: high and low  
 427 levels of resilience for both planktivorous fish and zooplankton. We define resilience of a stable  
 428 point as the distance (in units of the state variable) of a stable point from the unstable threshold  
 429 (Holling 1973). The different levels of resilience were achieved by adjusting  $s_2$  and  $k$ . In each  
 430 case, we solved for equilibria and computed eigenvalues for the linearization of the deterministic  
 431 skeleton of the model to confirm that there were three real roots, that the upper and lower roots  
 432 were stable, and that the middle root was unstable. In each of these four sets of simulations, we  
 433 computed variance for  $x_1$  alone (uncoupled from  $x_2$ ) and for the coupled system with three  
 434 different values for the correlation coefficient of shocks:  $r_{12} = -0.9, 0$  or  $+0.9$ . All other  
 435 parameter values were fixed for all simulations (Table 1). Parameter values were selected to  
 436 yield alternate state biomasses and thresholds similar to those obtained by Carpenter et al. (2008)  
 437 who fitted a model to field data from ecosystem experiments. We computed the amplification  
 438 index (left side of equation 7) and variance of both state variables. The variance was computed  
 439 for 1000 time steps near equilibrium using programs written in R (<http://www.r-project.org/>) by  
 440 S.R.C.  
 441

#### 442 *Negative Effect of $x_2$ on $x_1$*

443  
 444 Here we analyze the situation where planktivorous fish are near their lower stable point  
 445 and large-bodied zooplankton are near their higher stable point (Fig 4 A, C). When fishing  
 446 mortality of piscivores increases, planktivorous fish biomass increases. In the model,  $s_{2,t}$   
 447 increases thereby moving the lower stable point of  $x_2$  closer to the unstable threshold of  $x_2$ . Thus  
 448 resilience, in the sense of Holling (1973), of the lower stable point of  $x_2$  decreases. The increase  
 449 in  $\bar{x}_{2,t}$  causes  $s_{1,t}$  to decrease, thereby decreasing the resilience of the upper stable point of  $x_1$   
 450 (i.e. this upper stable point moves closer to the unstable threshold).  
 451

452 When  $k$  is negative, then  $\rho_{12}$  is negative because  $\rho_{12} = -k\bar{x}_1$ , from expression (2a).  
 453 Therefore we expect an inverse relationship between the amplification factor and  $r_{12}$ , the  
 454 correlation of the shocks, from equation (38)

455  
 456 First we examined the case when shock variances (diagonal elements of  $\Sigma$ ) are equal.  
 457 With equal shock variances and negative  $\rho_{12}$ , the amplification factor was positive for this  
 458 particular set of parameter values.

459  
 460 When resilience of both state variables was relatively high, variance was relatively low  
 461 and the amplification factor was near zero (Fig. 5A). The contrast is striking with the case in  
 462 which resilience of both state variables was relatively low (Fig. 5D). The amplification factor is  
 463 positive, indicating that variance is magnified by the dynamics of the interacting system. There is  
 464 a slight tendency for the amplification factor to decline as the correlation of shocks increases.  
 465 The variance of  $x_1$  alone (uncoupled from  $x_2$ ) is less than the variance observed for the coupled  
 466 system at any value of the correlation coefficient for shocks.

467  
 468 Variance also increased notably when resilience of zooplankton was decreased to a low  
 469 value while resilience of planktivores remained high (Fig. 5B). The amplification factor shows  
 470 that the system dynamics magnify the signal of the nearby threshold in zooplankton. The  
 471 amplification factor and the variance of  $x_1$  decline as the correlation of shocks increases. This  
 472 highlights the potential impact of correlated shocks on early warnings of critical transitions.

473  
 474 The case where planktivore resilience is low and zooplankton resilience is high shows  
 475 strongly muted variance of zooplankton (Fig. 5C). Indeed, variance of zooplankton is not  
 476 discernibly different from the case where both variables have high resilience (Fig. 5A). In  
 477 contrast, variance of planktivorous fish increased markedly in Fig. 5C compared to Fig. 5A. This  
 478 substantial increase in variance of planktivores was not expressed in the zooplankton. The  
 479 amplification factor was small. This example shows that the early warning of a nearby transition  
 480 in a predator may not be expressed in the variance of the prey.

481  
 482 We now turn to a case where the shock variance to zooplankton,  $\Sigma_{11}$ , is  $10^4$  larger than  
 483 shock variance to planktivorous fishes,  $\Sigma_{22}$  (Table 1). For the parameter values of this simulation,  
 484 the amplification factor is positive for negative  $r_{12}$ , and negative for positive  $r_{12}$ .

485  
 486 When resilience of both state variables was relatively high, variance was relatively low  
 487 and the amplification factor was near zero (Fig. 6A). The outcome was different when resilience  
 488 of both state variables was relatively low (Fig. 6D). The amplification factor is positive for  
 489 negative  $r_{12}$ , and negative for positive  $r_{12}$ . The variance of  $x_1$  and  $x_2$  is larger when both variables  
 490 have low resilience (Fig. 6D) than when the variables are farther away from their thresholds (Fig.  
 491 6A).

492  
 493 Variance of zooplankton,  $x_1$ , also increased when its resilience was decreased to a low  
 494 value while resilience of planktivores remained high (Fig. 6B). The amplification factor varies  
 495 inversely with  $r_{12}$ . However, the magnitude of muffling or magnifying is not large. Increased  
 496 variance of  $x_1$  signals the close approach of that variable to its threshold.

497

498 The case where planktivore ( $x_2$ ) resilience is low and zooplankton ( $x_1$ ) resilience is high  
 499 evoked low variance of zooplankton (Fig. 6C). Variance of zooplankton is not different from the  
 500 case where both variables have high resilience (Fig. 6A). In contrast, variance of planktivorous  
 501 fish increased. As in the case of equal variances, the early warning of a nearby transition in a  
 502 predator may not be expressed in the variance of the prey.

#### 504 *Positive Effect of $x_2$ on $x_1$*

506 To study responses with positive  $k$ , we analyzed the situation where planktivorous fish  
 507 are near their lower stable point and zooplankton are also near their lower stable point (Fig. 4  
 508 B,D). Instead of representing large-bodied zooplankton,  $x_1$  now represents small-bodied  
 509 zooplankton near their lower stable point. Biomass of small-bodied zooplankton is inversely  
 510 related to that of large-bodied zooplankton through the interactions described in Fig. 3. When  
 511 fishing mortality of piscivores increases, planktivorous fish biomass increases. In the model,  $s_{2,t}$   
 512 increases thereby moving the lower stable point of  $x_2$  closer to the unstable threshold of  $x_2$ . Thus  
 513 resilience of the lower stable point of  $x_2$  decreases. With positive  $k$ , the increase in  $\bar{x}_{2,l,t}$  causes  
 514  $s_{1,t}$  to increase, thereby decreasing the resilience of the lower stable point of  $x_1$  (i.e. this lower  
 515 stable point moves closer to the unstable threshold).

517 With  $k$  positive, we examined case where the shock variance to zooplankton,  $\Sigma_{11}$ , is  $10^4$   
 518 larger than shock variance to planktivorous fishes,  $\Sigma_{22}$ . In this situation the amplification factor  
 519 changes in the same direction as  $r_{12}$ : negative for negative  $r_{12}$ , and positive for positive  $r_{12}$ .

521 Results were rather similar to the cases described above (Fig. 7). The same three patterns  
 522 were evident. (1) Variance of each state variable increased as its resilience decreased. (2) The  
 523 amplification index responded as expected. However strong effects of muffling or magnification  
 524 were not evident. (3) In the case when planktivorous fish had low resilience but small-bodied  
 525 zooplankton had high resilience (Fig. 7C), neither the amplification index nor the zooplankton  
 526 variance changed appreciably, in comparison with the case where both state variables have high  
 527 resilience (i.e. compare Fig. 7A with Fig. 7C).

#### 529 DISCUSSION

531 In ecosystems subject to critical transitions, the approach to a regime shift can be  
 532 announced by increase of the autocorrelation coefficient toward one, increased variance or  
 533 skewness, or shift of the variance spectrum toward lower frequencies (Kleinen et al. 2003,  
 534 Carpenter and Brock 2006, Guttal and Jayaprakash 2008, van Nes and Scheffer 2007, Contamin  
 535 and Ellison 2009, Scheffer et al. 2009). These indicators may serve as diagnostics of critical  
 536 transitions in long-term observed data (Dakos et al. 2008). In management, the indicators may  
 537 reveal incipient regime shifts before they occur, allowing managers some time to take action to  
 538 avert unwanted regime shifts (Biggs et al. 2009, Contamin and Ellison 2009). Such applications  
 539 raise important questions about appropriate time series filters for data, statistical sensitivity of  
 540 indicators, the amount of time available to take effective action, and design of responsive  
 541 institutions (Kleinen et al. 2003, Carpenter and Brock 2006, Contamin and Ellison 2009, Biggs et  
 542 al. 2009). This paper addresses a different issue of interpreting variance shifts in ecosystems  
 543 subject to multiple critical transitions.

544  
 545  
 546  
 547  
 548  
 549  
 550  
 551  
 552  
 553  
 554  
 555  
 556  
 557  
 558  
 559  
 560  
 561  
 562  
 563  
 564  
 565  
 566  
 567  
 568  
 569  
 570  
 571  
 572  
 573  
 574  
 575  
 576  
 577  
 578  
 579  
 580  
 581  
 582  
 583  
 584  
 585  
 586  
 587  
 588

If the ecosystem is subject to two different but linked critical transitions, early warning indicators may behave in more complex or even counter-intuitive ways. This paper has investigated the interactions of regime shifts by focusing on variance in discrete-time models. We address variance because it is perhaps the simplest indicator to measure in field data, due to the availability of efficient estimators for small sample sizes.

As a discrete-time system approaches a critical point (specifically as the squared eigenvalue approaches one from below) the variance will increase from two distinct sources. The first source is the shift of the steady state variance  $\bar{\sigma}^2 = b^2 \text{var}(e_t) / (1 - \rho^2)$  toward infinity as the squared autocorrelation  $\rho^2$  approaches one from below. Theory and examples for this source of variance, or squealing, have been discussed elsewhere (Brock and Carpenter 2006, Brock et al. 2008, Carpenter and Brock 2006, Biggs et al. 2009, Scheffer et al. 2009).

The second source of variance, flickering, can occur if the range of the noise is large enough to occasionally push the system across a critical threshold. This shock-driven shift may be temporary, if subsequent shocks move the system back to the original attractor, or persistent if subsequent shocks move the system back to the original attractor. Scheffer et al. (2009) noted the distinction between flickering and squealing but did not pursue the idea in detail. Flickering may be more important in discrete-time models, where it is possible to jump across thresholds, than in continuous time models where dynamics are very slow near thresholds. Nonetheless, flickering occurs in a continuous-time model of lake dynamics subject to relatively small shocks to nutrient recycling and relatively larger shocks to nutrient input from the watershed (Carpenter and Brock 2006). In the paleoclimate record, transitions between century-scale cold and warm periods are marked by rapid transitions between dusty and dust-free conditions, with as many as four such flickers preceding each transition (Taylor et al. 1993). During the transition from anaerobic to aerobic earth, about 2.7 to 2.3 billion years ago, three flickers of oxygenation of the atmosphere seem to have occurred before planetary primary production rates became high enough to maintain an oxygenated atmosphere (Godfrey and Falkowski 2009).

Ecosystem dynamics can muffle or magnify variance due to a nearby critical transition. The effect of ecosystem dynamics depends on the interaction between the state variables that are subject to critical transitions. For two variables, each subject to a critical transition, the effect on variance depends on the sign of the interaction between the variables ( $\rho_{12}$ ) multiplied by the sign of the correlation of the response of the variables to environmental shocks ( $r_{12}$ ). In a predator-prey or competitive relationship the sign of the interaction will be negative. Correlation of the response to environmental shocks is less obvious. It is easy to think of cases where both species respond in the same direction to a given shock, as well as cases where species respond oppositely to a given shock.

If the sign of  $\rho_{12}r_{12}$  is positive, then ecosystem interactions magnify the variance. Such interactions increase the intensity of the early warning of an impending regime shift. For a predator-prey interaction, magnification will occur if the two species have opposite responses to environmental variability.

589           If the sign of  $\rho_{12}r_{12}$  is negative, then ecosystem interactions can muffle or magnify the  
590 variance, depending on the relative magnitudes of the terms in equation (38). If muffling occurs,  
591 the signal of an impending regime shift would be muted, and perhaps obscure an early warning.  
592 For a predator-prey interaction, muffling will occur if the two species have respond in the same  
593 direction to environmental variability.

594  
595           Our findings complement studies of the effect of correlated and autocorrelated  
596 environmental noise on linear ecological systems (Ripa and Ives 2003, 2007). Correlated and  
597 autocorrelated environmental shocks can have large effects that are not intuitive. For example  
598 they can dampen or intensify predator-prey cycles (Ripa and Ives 2003). Because environmental  
599 correlations and autocorrelations can dampen or intensify dynamical patterns, underlying  
600 phenomena such as predation and competition can become less or more detectable in long-term  
601 data (Ripa and Ives 2007). Thus the interaction of environmental noise with ecosystem processes  
602 poses profound challenges for inferring ecological interactions from time-series data.

603  
604           As our simulations show, ecosystem interactions can suppress the expression of an early  
605 warning for an impending regime shift. Early warnings were weakest in cases where predator  
606 resilience was low yet prey resilience was high (Figs. 5C, 6C, 7C). This outcome suggests a  
607 mechanism for false negatives in early warning signals based on variance. On the other hand,  
608 early warning signals were strongly expressed in fishes when their resilience was low, and in  
609 zooplankton when their resilience was low.

610  
611           Other models of lake food webs have demonstrated rather strong transmission of variance  
612 (Carpenter 1988) including in situations where variance is generated by an approaching critical  
613 transition (Carpenter et al. 2008). In these cases, unlike the present case, a nonlinearity in top  
614 predators was linked to a linear food chain. In this paper we consider a food web with two  
615 critical transitions. Even though low resilience in a predator increases variance in the predator  
616 biomass, this variance is not necessarily transmitted to the prey if the prey resilience is high.

617  
618           Another cause of low variance transmission in these simulations is the very small  
619 magnitude of the shock variances relative to the resilience of the state variables. Simulations  
620 used small shock variances and rather high resilience in order to sample the stationary  
621 distribution for long periods of time without causing a regime shift by flickering. In nature,  
622 shocks could be larger in relation to resilience, and flickering could lead to much larger changes  
623 in variance. Of course such flickering could also trigger regime shifts.

624  
625           Nonetheless, muffling and magnification should be considered in applications of early  
626 warnings for ecosystem regime shifts. The magnitude depends in complicated ways on the  
627 structure and parameters of the ecosystem model under study. While our analyses suggest the  
628 potential importance of muffling and magnification in the dynamics of ecosystems subject to  
629 multiple kinds of critical transitions, individual cases may show unique patterns.

630  
631           The conditions for muffling versus magnification suggest a straightforward solution for  
632 the dangers of variance muffling in field studies. Measurements should be made for two state  
633 variables, one that has a negative link to the critical transition and one that has a positive link to  
634 the critical transition. The critical transition of planktivorous fishes in our example has a negative

635 effect on large-bodied herbivores but a positive effect on small-bodied herbivores. Thus large-  
 636 and small-bodied herbivores have oppositely-signed values for  $\rho_{12}$ . Therefore at least one group  
 637 of herbivores will magnify the early warning, provided that the sign of  $r_{12}$  is the same for both  
 638 groups of herbivores. As a general rule for ecosystem monitoring, one should plan to measure  
 639 variables that are likely to have opposite responses to the regime shifts of interest.

640  
 641 Muffling and magnification have a further important implication for regime shifts, one  
 642 that is distinct from their role in early warnings. Flickering may trigger regime shifts. A review  
 643 of case studies (Scheffer et al. 2002) argued that many cases of regime shifts in ecosystems were  
 644 caused by random shocks to systems with low resilience. Results presented here show that  
 645 interactions of different critical transitions in an ecosystem affect the susceptibility of the  
 646 ecosystem to regime shifts caused by shocks. Conditions that increase muffling will decrease the  
 647 chance of regime shifts caused by shocks. Conversely, conditions that increase magnification  
 648 will increase the chance of regime shifts caused by shocks. Therefore, muffling and  
 649 magnification must be considered when evaluating the risk that a system will undergo a regime  
 650 shift due to random shocks. Expanding linkages among climate, ecosystems, human health and  
 651 the economy may increase the frequency of connected global regime shifts in the future (Walker  
 652 et al. 2009). Where these are linked by positive feedbacks and have positive correlations to  
 653 exogenous shocks there is greater chance of cascading regime shifts.

654  
 655 It is likely that many complex systems have the potential for regime shifts (Scheffer  
 656 2009). Some kinds of regime shifts are known, even if thresholds are hard to predict, but other  
 657 types of regime shifts are as yet unknown. In view of the rich complexities of environmental  
 658 systems, it is likely that many links among critical transitions can occur. Scientists attempting to  
 659 understand these phenomena are in the early days of a complex and challenging enterprise.  
 660 Further development and evaluation of regime shift indicators will require careful system-  
 661 specific modeling combined with detailed data-based field investigation.

#### 662 ACKNOWLEDGEMENTS

663  
 664 Tony Ives, Mike Pace and Marten Scheffer provided helpful comments on the manuscript. We  
 665 thank Aaron Ellison, Simon Levin and an anonymous referee for thoughtful reviews. This work  
 666 was supported by NSF grants to S.R.C. W.A.B. acknowledges support by NSF and the Vilas  
 667 Trust.  
 668

#### 669 LITERATURE CITED

670  
 671 Biggs, R., S.R. Carpenter and W.A. Brock. 2009. Turning back from the brink: Detecting an  
 672 impending regime shift in time to avert it. *Proceedings of the National Academy of Sciences*  
 673 106: 826-831.  
 674

675  
 676 Brock, W. A. and S. R. Carpenter 2006. Variance as a leading indicator of regime shift in  
 677 ecosystem services. *Ecology and Society* 11 (2): 9. [online] URL:  
 678 <http://www.ecologyandsociety.org/vol11/iss2/art9/>  
 679

- 680 Brock, W.A., S.R. Carpenter, and M. Scheffer. 2008. Regime shifts, environmental signals,  
681 uncertainty and policy choice. p. 180-206 in J. Norberg and G. Cumming (eds.), A theoretical  
682 framework for analyzing social-ecological systems. Columbia, NY, USA.
- 683  
684 Carpenter, S.R. 2002. Ecological futures: building an ecology of the long now. *Ecology* 83:  
685 2069-2083.
- 686  
687 Carpenter, S.R. 2003. Regime shifts in lake ecosystems: Pattern and variation. Ecology Institute,  
688 Oldendorf/Luhe, Germany.
- 689  
690 Carpenter, S.R. and W.A. Brock. 2006. Rising variance: A leading indicator of ecological  
691 transition. *Ecology Letters* 9: 311-318.
- 692  
693 Carpenter, S.R., W.A. Brock, J.J. Cole, J.F. Kitchell and M.L. Pace. 2008. Leading indicators of  
694 trophic cascades. *Ecology Letters* 11: 128-138.
- 695  
696 Carpenter, S.R. and J.F. Kitchell (eds.). 1993. The trophic cascade in lakes. Cambridge  
697 University Press, Cambridge, England.
- 698  
699 Carpenter, S.R. and R.C. Lathrop. 2008. Probabilistic estimate of a threshold for eutrophication.  
700 *Ecosystems* 11: 601-613.
- 701  
702 Contamin, R. and A.M. Ellison. 2009. Indicators of regime shifts in ecological systems: what do  
703 we need to know and when do we need to know it? *Ecological Applications* 19: 799-816.
- 704  
705 Dakos, V., M. Scheffer, E.H. van Nes, V. Brovkin, V. Petoukhov and H. Held. 2008. Slowing  
706 down as an early warning system for abrupt climate change. *Proceedings of the National*  
707 *Academy of Sciences* 105: 14308-14312.
- 708  
709 Dodson, S.I. 1974. Zooplankton competition and predation: an experimental test of the size-  
710 efficiency hypothesis. *Ecology* 55: 605-613.
- 711  
712 Dushoff, J., J. Plotkin, S. Levin, D. Earn. 2004. Dynamical resonance can account for seasonality  
713 of influenza epidemics. *Proceedings of the National Academy of Sciences* 101: 16915-16916.
- 714  
715 Godfrey, L.V. and P.G. Falkowski. 2009. The cycling and redox state of nitrogen in the Archean  
716 ocean. *Nature Geosciences* 2: 725-729.
- 717  
718 Guttal V, Jayaprakash C. 2008. Changing skewness: an early warning signal of regime shifts in  
719 ecological systems. *Ecology Letters* 11: 450-460.
- 720  
721 Hall, D.J., S.T. Threlkeld, C.W. Burns and P.H. Crowley. 1976. The size-efficiency hypothesis  
722 and the size structure of zooplankton communities. *Annual Review of Ecology and Systematics*  
723 7: 177-208.
- 724

- 725 Holling, C.S. 1973. Resilience and stability of ecological systems. *Annual Review of Ecology*  
726 *and Systematics* 4: 1-23.  
727
- 728 Ives, A.R. and S.R. Carpenter. 2007. Stability and diversity of ecosystems. *Science* 317: 58-62.  
729
- 730 Ives, A.R., B. Dennis, K.L. Cottingham and S.R. Carpenter. 2003. Estimating community  
731 stability and ecological interactions from time-series data. *Ecological Monographs* 73: 301-330.  
732
- 733 Jeppesen, E., M. Sondergaard, M. Sondergaard, and K. Christofferson (eds.) 1998. The  
734 structuring role of submerged macrophytes in lakes. Springer-Verlag, Berlin.  
735
- 736 Kerfoot, W.C. 1980. Evolution and ecology of zooplankton communities. University Press of  
737 New England, Hanover, New Hampshire, USA.  
738
- 739 Kleinen, T., H. Held, and G. Petschel-Held. 2003. The potential role of spectral properties in  
740 detecting thresholds in the earth system: application to the thermohaline circulation. *Ocean*  
741 *Dynamics* 53: 53-63.  
742
- 743 MA (Millennium Ecosystem Assessment). 2005. Ecosystems and human well-Being: Our  
744 human planet: Summary for decision makers. Island Press, Washington D.C.  
745
- 746 May, R.M. and A. McLean (eds.). 2007. *Theoretical Ecology: Principles and Applications*.  
747 Oxford University Press, Oxford, U.K.  
748
- 749 Narisma, G.T., J.A. Foley, R. Licker, and N. Ramankutty. 2007. Abrupt changes in rainfall  
750 during the twentieth century. *Geophysical Research Letters* 34, L06710,  
751 doi:10.1029/2006GL028628.  
752
- 753 Neill, W.E. 1975. Experimental studies of microcrustacean competition, community composition  
754 and efficiency of resource utilization. *Ecology* 56: 809-826.  
755
- 756 Neill, W.E. 1988. Complex interactions in oligotrophic lake food webs: Responses to nutrient  
757 enrichment. pp. 31-44 in S.R. Carpenter (ed.), *Complex Interactions in Lake Communities*.  
758 Springer-Verlag, NY.  
759
- 760 Persson, L., P.-A. Amundsen, A.M. De Roos, A. Klemetsen, R. Knudsen, and P. Primicerio.  
761 2007. Culling prey promotes predator recovery – alternative states in a whole-lake experiment.  
762 *Science*, 316: 1743-1746.  
763
- 764 Peters, D.P.C., R.A. Pielke Sr., B.T. Bestelmeyer, C.D. Allen, S Munson-McGee, S. and K.M.  
765 Havstad. 2004. Cross-scale interactions, nonlinearities, and forecasting catastrophic events.  
766 *Proceedings of the National Academy of Sciences* 101: 15130-15135.  
767
- 768 Petraitis, P.S. and R.E. Latham. 1999. The importance of scale in testing the origins of  
769 alternative community states. *Ecology* 80: 429-442.  
770

- 771 Rietkerk M., S.C. Dekker, P.C. de Ruiter, and J. van de Koppel. 2004. Self-organized patchiness  
772 and catastrophic shifts in ecosystems. *Science* 305: 1926-1929.  
773
- 774 Ripa, J., and A. R. Ives. 2003. Food web dynamics in correlated and autocorrelated  
775 environments. *Theoretical Population Ecology* 64:369-384.  
776
- 777 Ripa, J., and A. R. Ives. 2007. Interaction assessments in correlated and autocorrelated  
778 environments. In D. A. Vasseur, and K. S. McCann, eds., *The impact of*  
779 *environmental variability on ecological systems*. Springer, Dordrecht, Germany.  
780
- 781 Schaffer, W.M., B.S. Pederson, B.K. Moore, O. Skarpaas, A.A. King, T.V. Bronnikova. 2001.  
782 Sub-harmonic resonance and multi-annual oscillations in northern mammals: a nonlinear  
783 dynamical systems perspective. *Chaos, Solitons and Fractals*, 12, 251-264.  
784
- 785 Scheffer, M. 1997. *The ecology of shallow lakes*. Chapman and Hall, London.  
786
- 787 Scheffer, M. 2009. *Critical transitions in nature and society*. Princeton University Press,  
788 Princeton, NJ, USA.  
789
- 790 Scheffer, M., J. Bascompte, W.A. Brock, V. Brovkin, S.R. Carpenter, V. Dakos, H. Held, E.H.  
791 Van Nes, M. Rietkerk and J. Sugihara. 2009. Early warning signals for critical transitions. *Nature*  
792 461: 53-59.  
793
- 794 Scheffer, M. and S.R. Carpenter. 2003. Catastrophic regime shifts in ecosystems: linking theory  
795 to observation. *Trends in Ecology and Evolution* 12: 648-656.  
796
- 797 Scheffer, M., S. Carpenter, J. Foley, C. Folke and B. Walker. 2001. Catastrophic shifts in  
798 ecosystems. *Nature* 413: 591-596.  
799
- 800 Scheffer, M., Rinaldi, S. and Kuznetsov, Y.A. 2000. The effect of fish on plankton dynamics: a  
801 theoretical analysis. *Canadian Journal of Fisheries and Aquatic Sciences* 57: 1208-1219.  
802
- 803 Schmitz, O.J., E.L. Kalies, and M.G. Booth. 2006. Alternative dynamic regimes and trophic  
804 control of plant succession. *Ecosystems* 9: 659-672.  
805
- 806 Taylor, K.C., G.W. Lamory, G.A. Doyle, R.B. Alley, P.M. Grootes, P.A. Mayewski,  
807 J.W.C. White and K.L. Barlow. 1993. The 'flickering switch' of late Pleistocene climate change.  
808 *Nature* 361: 432-436.  
809
- 810 Ursin, E. 1982. Stability and variability in the marine ecosystem. *Dana* 2: 51-65.  
811
- 812 van Nes, E. and M. Scheffer. 2007. Slow recovery from perturbations as a generic indicator of a  
813 nearby catastrophic shift. *The American Naturalist* 169: 738-747.  
814

- 815 Walker, B. and J.A. Meyers. 2004. Thresholds in ecological and social-ecological systems: A  
816 developing database. *Ecology and Society* 9(2):3, URL:  
817 <http://www.ecologyandsociety.org/vol9/iss2/art3>  
818
- 819 Walker, B., S. Barrett, S. Polasky, V. Galaz, C. Folke, G. Engstrom, F. Ackerman, K. Arrow, S.  
820 Carpenter, K. Chopra, G. Daily, P. Ehrlich, T. Hughes, N. Kautsky, S. Levin, K-G. Maler, J.  
821 Shogren, J. Vincent, T. Xepapadeas and A. de Zeeuw. 2009. Looming global-scale failures and  
822 missing institutions. *Science* 325: 1345-1346.  
823
- 824 Walters, C. and J.F. Kitchell. 2001. Cultivation/depensation effects on juvenile survival and  
825 recruitment: implications for the theory of fishing. *Canadian Journal of Fisheries and Aquatic*  
826 *Sciences* 58: 39-50.  
827
- 828 Walters, C.J. and S.J.D. Martell. 2004. *Fisheries ecology and management*. Princeton University  
829 Press, Princeton, N.J.  
830
- 831 Wiesenfeld K, Moss F. 1995. Stochastic resonance and the benefits of noise: from ice ages to  
832 crayfish and SQUIDS. *Nature* **373**: 33–36.  
833
- 834 Weitzman, M. 2009. On modeling and interpreting the dynamics of catastrophic climate change.  
835 *Review of Economics and Statistics* 91: 1-19.  
836

837 Table 1. Symbols used in the equations in the text.  
838

Symbol	Definition	Numerical Values
$a$	equilibrium values for unforced dynamics	For $x_1$ : $a_l=1, a_c=3, a_u=6$ For $x_2$ : $a_l=0.25, a_c=1, a_u=2.5$
$b$	effect of a shock	
$c$	rate coefficient	For $x_1$ : 0.015 For $x_2$ : 0.2
$e$	random variable, where $\{e_{it}\}$ is a stationary sequence of random variables, each with mean zero and variance $\sigma_e^2$	
$E$	expectation operator	
$f$	rate function for state variable $i$	
$f_{y_i}$	derivative of a rate function w.r.t. $x$ , evaluated at $y_i$	
$k$	effect of $x_2$ on the slow variable that forces $x_1$	scenarios with negative $k$ : -0.01, -0.48, -0.2, or -0.25 scenarios with positive $k$ : 0.06, 0.23, 0.06, or 0.12
$M$	steady-state moment matrix $M := E_{\infty} y_t y_t'$	
$N$	IID multivariate noise process with variance-covariance matrix $\Sigma$	
$n$	shock effect; $n_{i,t+1} := b_{i1}e_{1,t+1} + b_{i2}e_{2,t+1}$ , $i=1,2$	
$o(.)$	higher-order terms from a Taylor expansion	
$r_{12}$	correlation coefficient of shocks to $x_1$ and $x_2$ ; $r_{12} := \Sigma_{12} / (\Sigma_{1,1}^{0.5} \Sigma_{2,2}^{0.5})$	-0.9, 0 or +0.9
$s_1$	slow variable that affects $x_1$	
$s_2$	slow variable that forces $x_2$	0 or 0.48, depending on the scenario
$x$	state variable	
$y$	small deviation of a state variable from equilibrium	
$\rho$	first-order terms of a Taylor expansion	
$\Sigma$	variance-covariance matrix of shocks	$\text{var}(x_1) = 10^{-5}$ ; $\text{var}(x_2) = 10^{-5}$ or $10^{-9}$ as specified; covariance computed from $r_{12}$

Figure 1.  $x_{t+1}$  versus  $x_t$  for a system with three equilibria (black curve) showing upper and lower bounds for the stochastic shocks (gray curves). Dotted line shows  $x_{t+1} = x_t$ . The upper and lower equilibria are stable and the middle equilibrium is an unstable threshold. (A) Base case. (B) Squealing: the curve has moved upward a small amount. Variance of  $x_{t+1}$  increases near the lower equilibrium. This increase, called squealing, is related to the change in slope (eigenvalue) of the curve where it crosses the diagonal line (see text). (C) Flickering and squealing: the curve has moved upward farther. Flickering – shocks that move the system across the unstable threshold – can occur. (D) After the regime shift: the curve has moved so far upward that only the upper stable equilibrium is attainable.

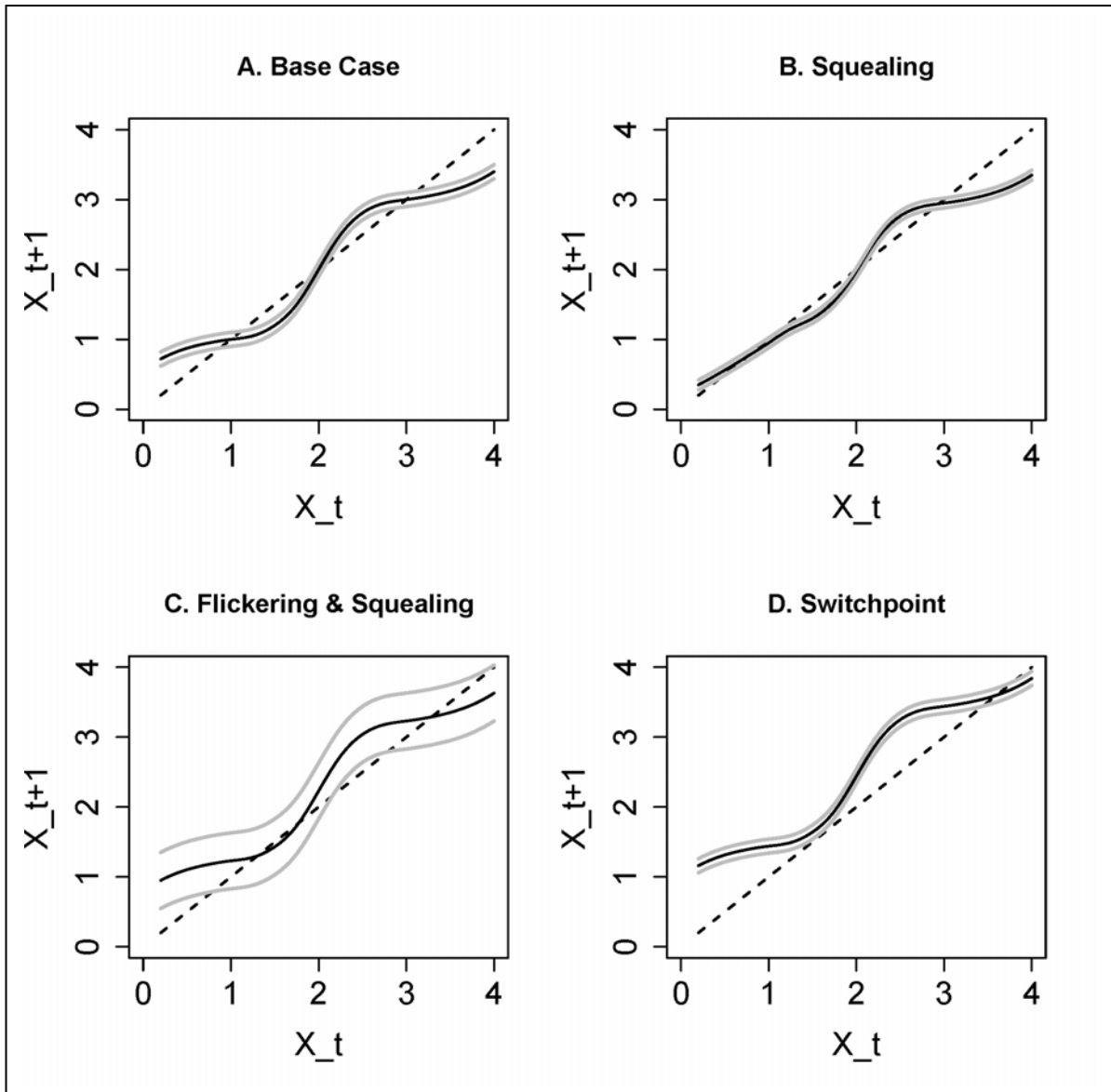


Figure 2. Flickering in the simplified linear model. (A) Model with positive slopes. (B) Model with zero slopes.

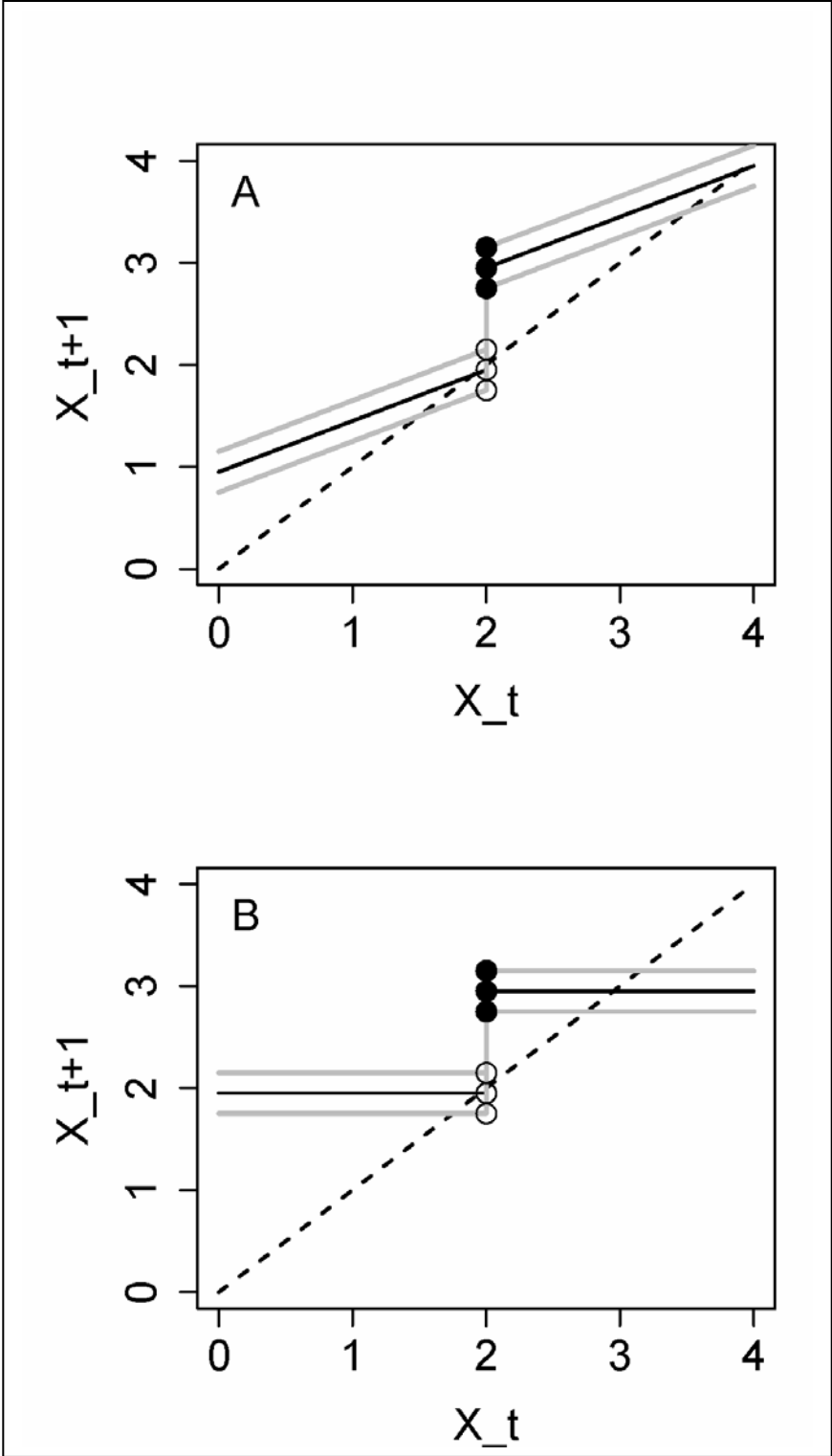


Figure 3. Trophic connections (solid lines) in the pelagic foraging arena of a lake, showing subsidies from terrestrial and littoral prey (dotted lines) and connections to littoral and deep-water refuges (dashed lines). The trophic triangle involving adult bass, golden shiners and juvenile bass is shaded gray. The trophic triangle involving phantom midge, large-bodied *Daphnia*, and small-bodied grazers is cross-hatched.

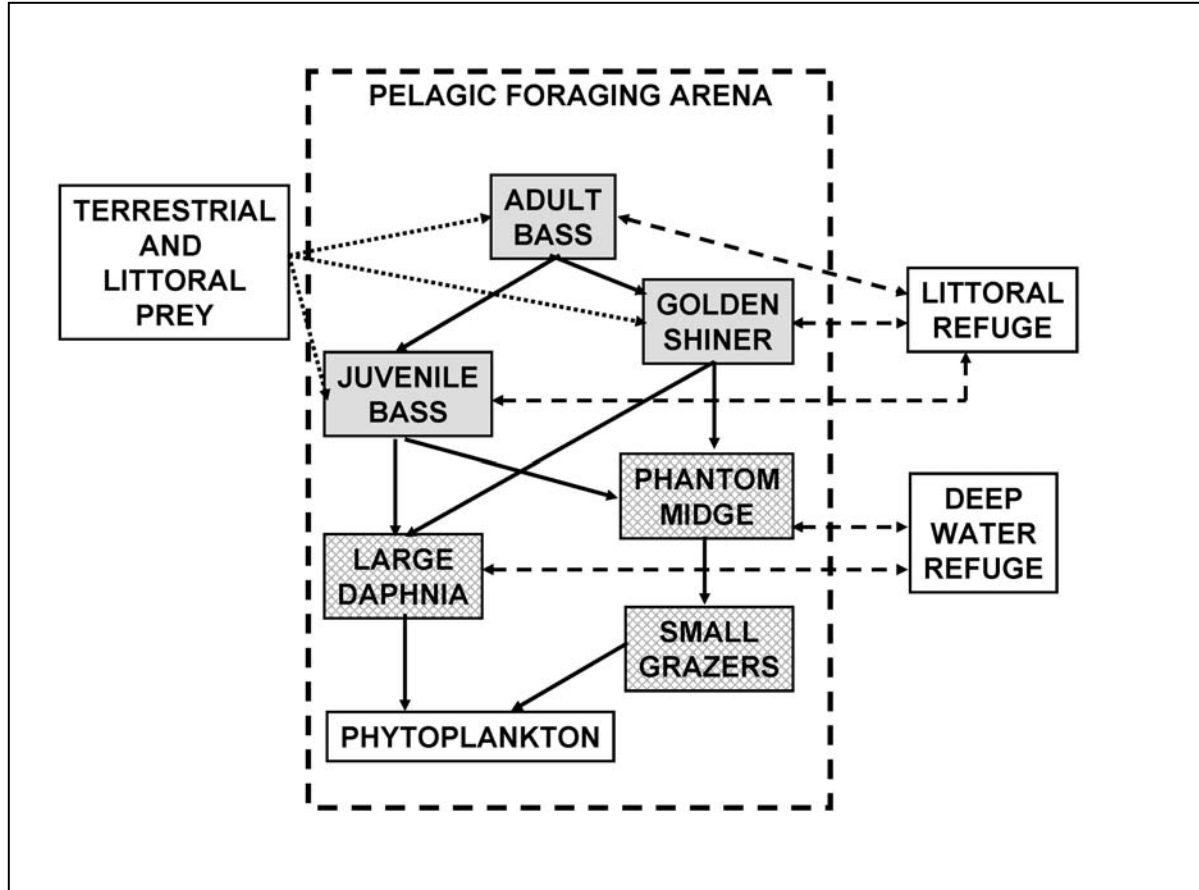


Figure 4. Changes in stability used in the simulations. Top row is  $x_2$  (planktivorous fishes) and bottom row is  $x_1$  (zooplankton). Left column depicts scenarios with negative  $k$  ( $x_1$  represents large-bodied zooplankton), right column depicts scenarios with positive  $k$  ( $x_1$  represents small-bodied zooplankton). Dashed lines were computed with  $s_2 = 0$ , solid lines were computed with  $s_2 = 0.4$ . (A) and (B) note decreased resilience of the lower equilibrium for  $x_2$  as  $s_2$  increases. (C) Note decreased resilience of the upper equilibrium for  $x_1$  as  $s_2$  increases. (D) Note decreased resilience of the lower equilibrium of  $x_1$  as  $s_2$  increases.

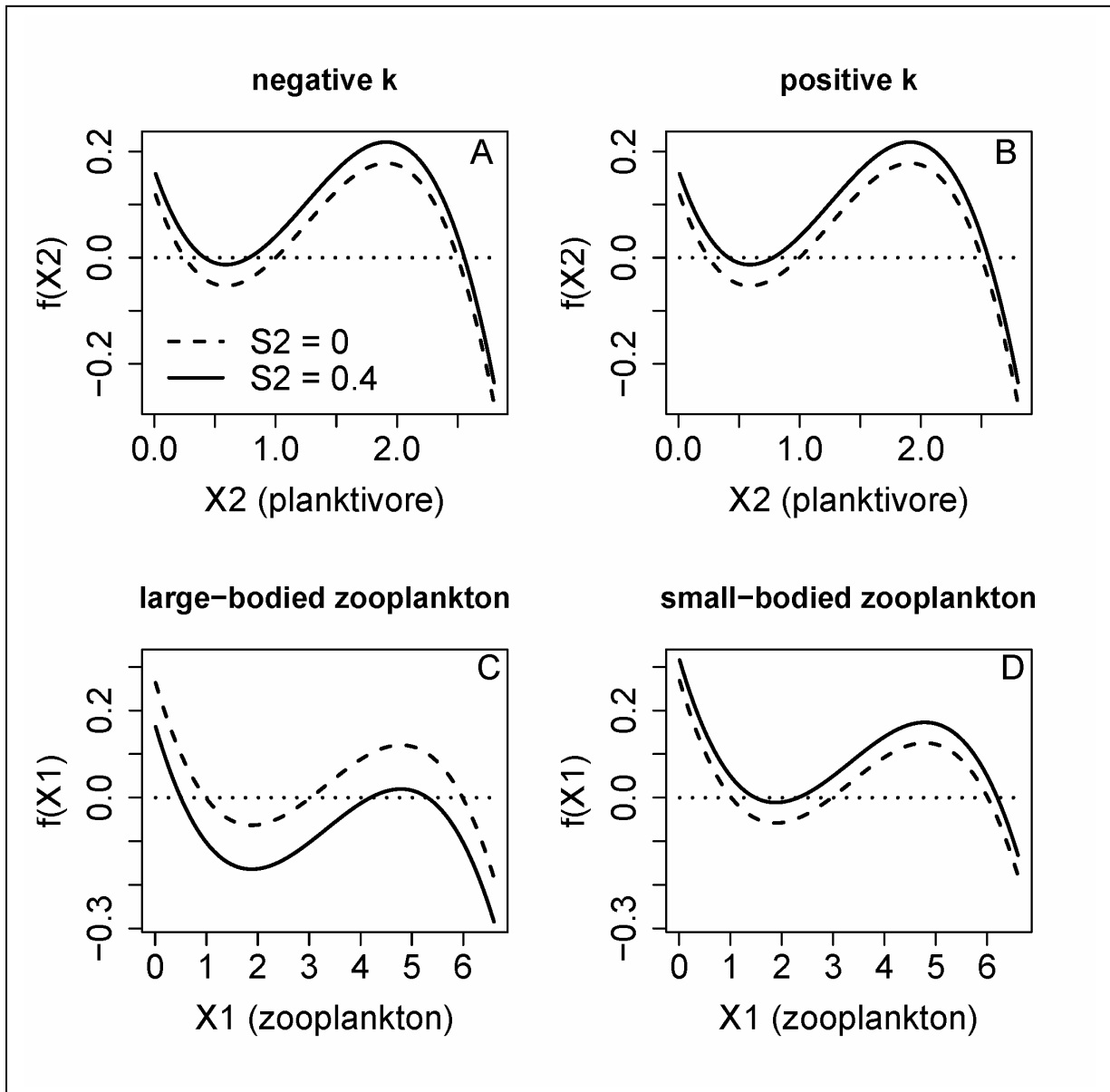


Figure 5. Variance and amplification factors when  $x_2$  has a negative effect on  $x_1$  and the variance of shocks to  $x_1$  is equal to the variance of shocks to  $x_2$ . Variance of  $x_{1,t}$ , variance of  $x_{2,t}$  (multiplied by  $10^5$ ) and amplification indicator (multiplied by  $10^3$ ) are presented. Each panel shows outcomes for  $x_{1,t}$  alone (uncoupled from  $x_2$ ) and for the coupled system with three correlation coefficients for the shocks ( $r_{12} = -0.9, 0$  or  $0.9$ ). (A)  $x_1$  and  $x_2$  far from their respective unstable thresholds (high resilience). (B) Low resilience of  $x_1$ , high resilience of  $x_2$ . (C) High resilience of  $x_1$ , low resilience of  $x_2$ . (D) Low resilience of  $x_1$  and  $x_2$ .

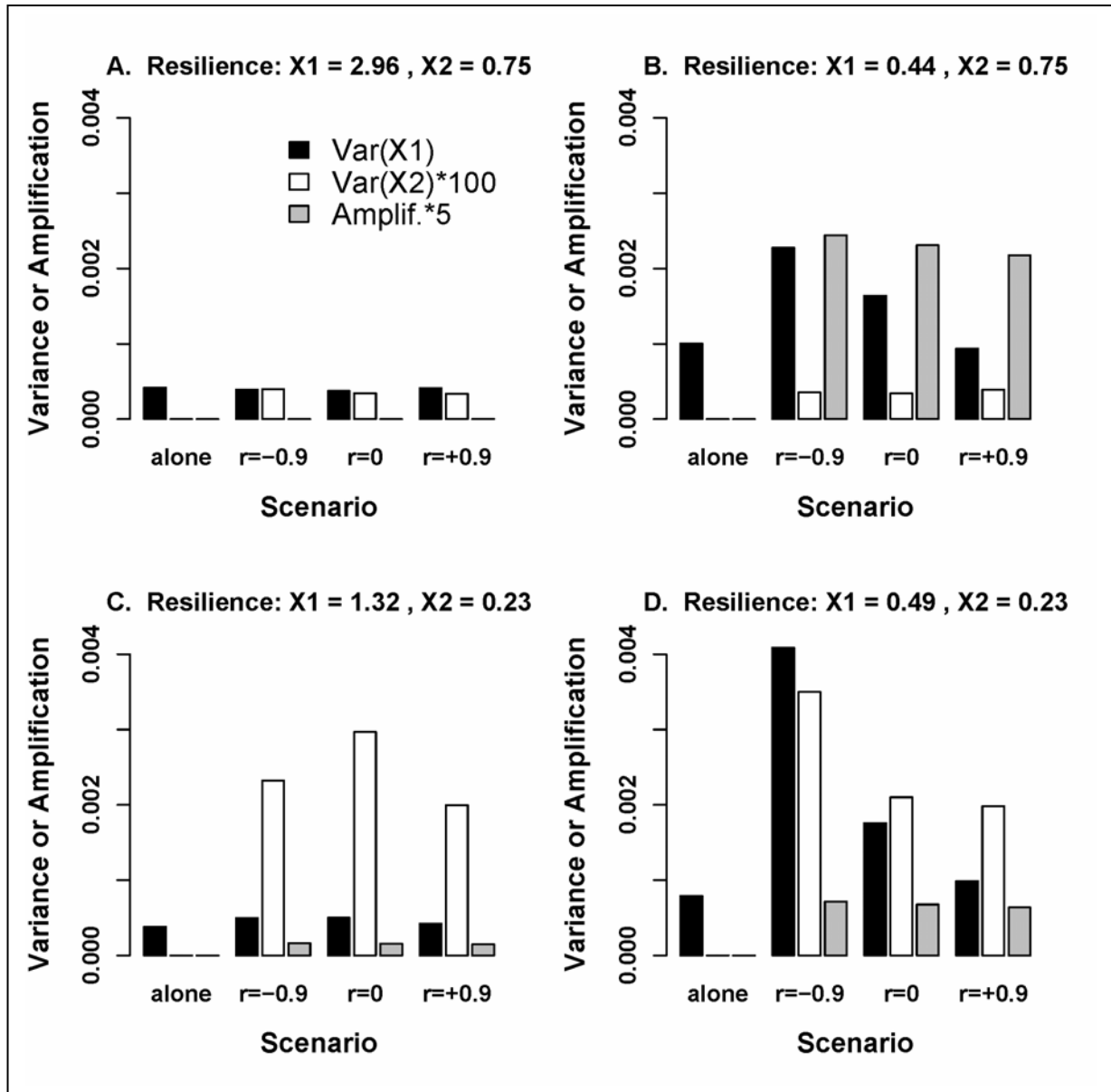


Figure 6. Variance and amplification factors for simulated scenarios when  $x_2$  has a negative effect on  $x_1$  and the variance of shocks to  $x_1$  is much larger than the variance of shocks to  $x_2$ . Variance of  $x_{1,t}$ , variance of  $x_{2,t}$  (multiplied by  $10^5$ ) and amplification indicator (multiplied by  $10^3$ ) are presented. Each panel shows outcomes for  $x_{1,t}$  alone (uncoupled from  $x_2$ ) and for the coupled system with three correlation coefficients for the shocks ( $r_{12} = -0.9, 0$  or  $0.9$ ). (A)  $x_1$  and  $x_2$  far from their respective unstable thresholds (high resilience). (B) Low resilience of  $x_1$ , high resilience of  $x_2$ . (C) High resilience of  $x_1$ , low resilience of  $x_2$ . (D) Low resilience of  $x_1$  and  $x_2$ .

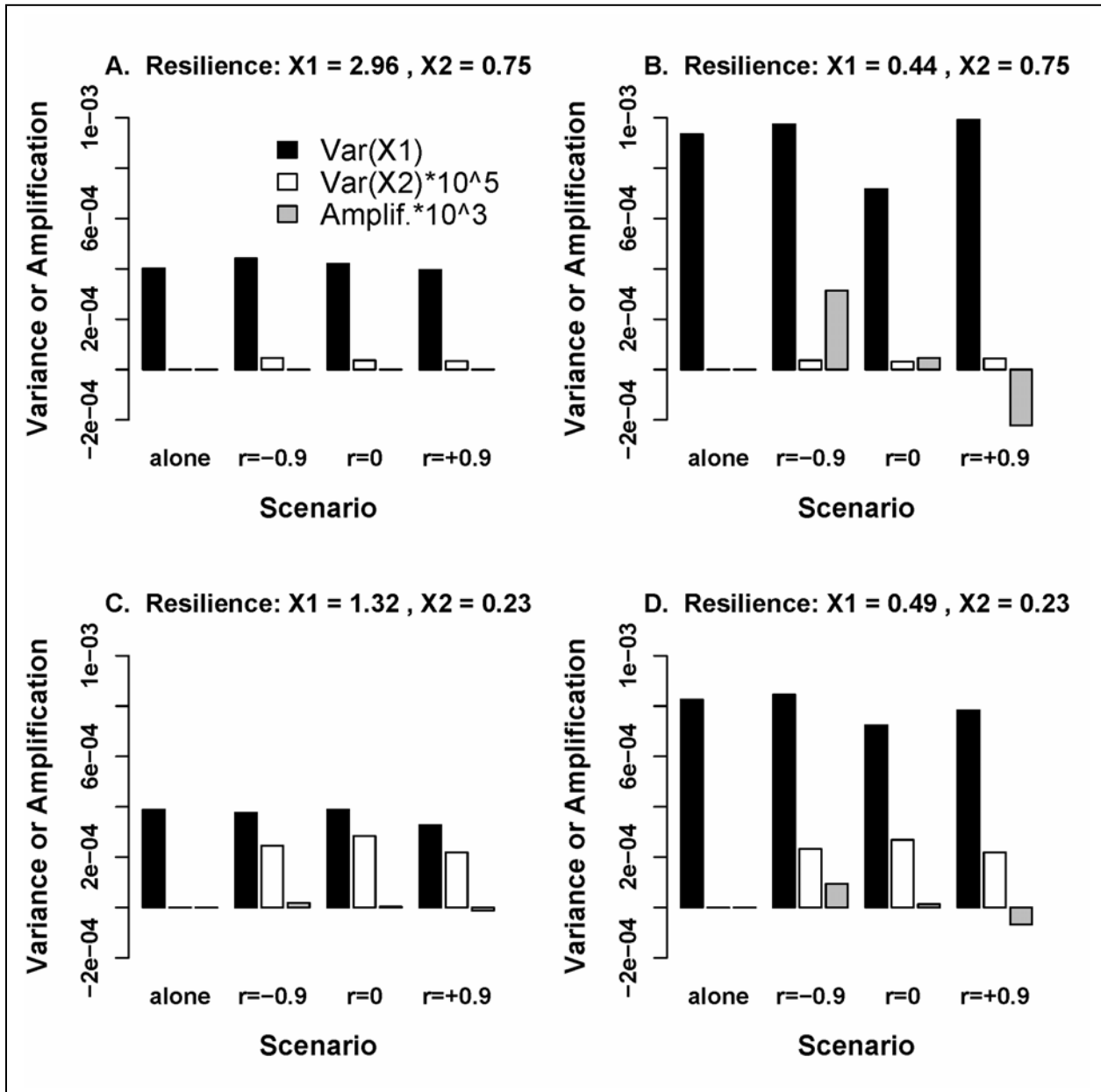
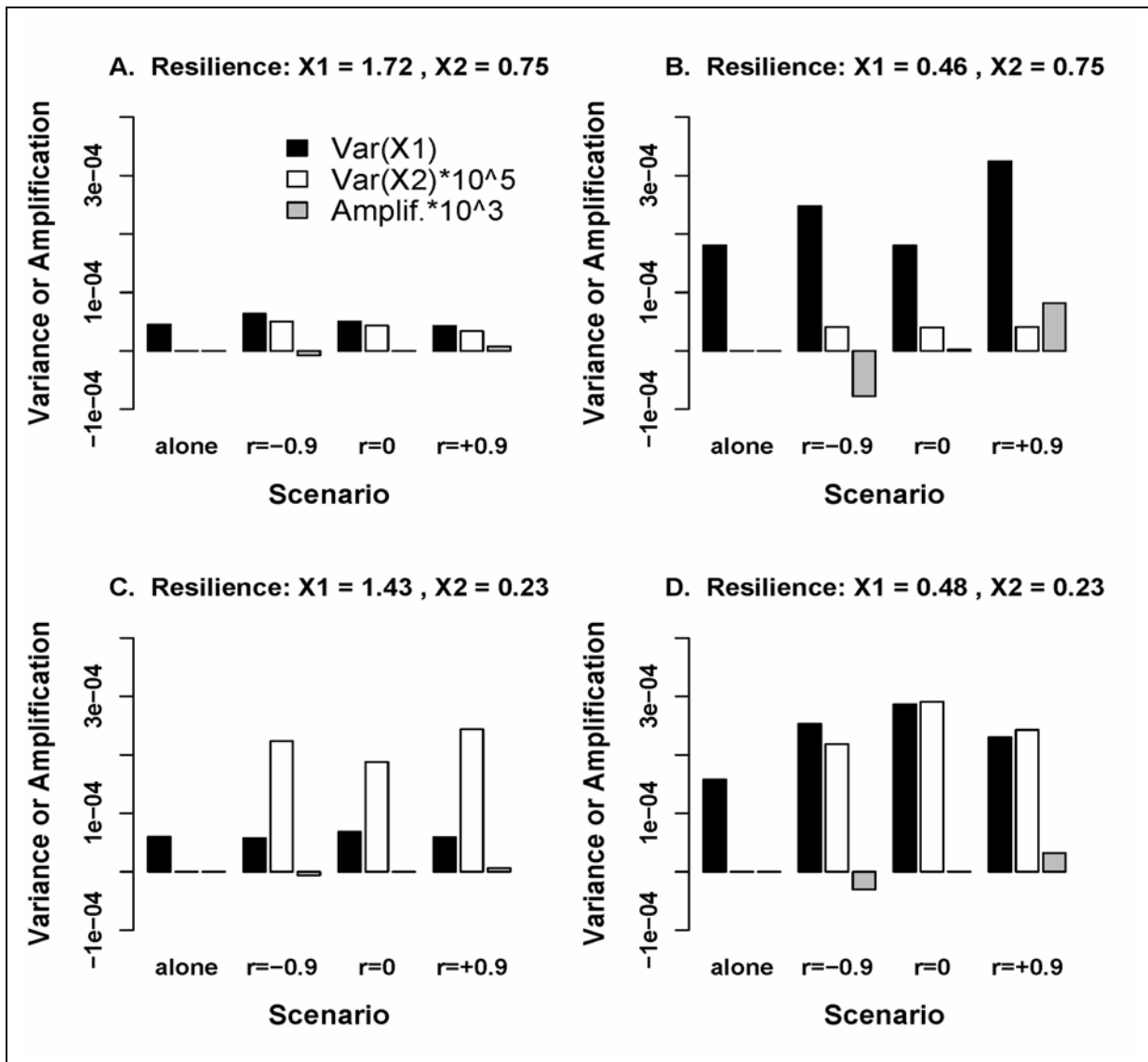


Figure 7. Variance and amplification factors for simulated scenarios when  $x_2$  has a positive effect on  $x_1$  and the variance of shocks to  $x_1$  is much larger than the variance of shocks to  $x_2$ . Variance of  $x_{1,t}$ , variance of  $x_{2,t}$  (multiplied by  $10^5$ ) and amplification indicator (multiplied by  $10^3$ ) are presented. Each panel shows outcomes for  $x_{1,t}$  alone (uncoupled from  $x_2$ ) and for the coupled system with three correlation coefficients for the shocks ( $r_{12} = -0.9, 0$  or  $0.9$ ). (A)  $x_1$  and  $x_2$  far from their respective unstable thresholds (high resilience). (B) Low resilience of  $x_1$ , high resilience of  $x_2$ . (C) High resilience of  $x_1$ , low resilience of  $x_2$ . (D) Low resilience of  $x_1$  and  $x_2$ .



1 **Conditions for Muffling or Magnifying Variance in**  
 2 **Ecosystems With Multiple Regime Shifts**

3  
 4 Appendix to

5  
 6 “Interacting Regime Shifts in Ecosystems: Implications for Early Warnings”

7 by

8 W.A. Brock and S.R. Carpenter

9  
 10  
 11 INTRODUCTION

12  
 13 The purpose of this Appendix is to explain the conditions for muffling or magnifying  
 14 variance when regime shifts interact, using a framework that is more general than the ecological  
 15 case study presented in the main text.

16  
 17 SQUEALING AND FLICKERING

18  
 19 We need to fix some mathematical ideas that will be used in the models below. In order  
 20 to do this we use a minimal model that is rather abstract. However this model is complex enough  
 21 to define squealing and flickering precisely, which is necessary in order to account for their  
 22 effects on variance when regime shifts interact. It may be helpful to the reader to look at Figures  
 23 1 and 2 of the main text as we explain equations (1)-(4) below. We introduce these ideas by first  
 24 using the following one dimensional stochastic dynamical system in discrete time (t),  
 25

26 (1)  $x_{t+1} = \bar{a} + s_1(t\varepsilon_1) + \rho(s_2(t\varepsilon_2))x_t + be_{t+1} + \beta I[x_t \geq x_c], t = 1, 2, \dots$   
 27  $x_1$  given by history,

28 Equation (1) is a simple linear autoregressive process driven by uncorrelated shocks  $\{e_t\}$  and a  
 29 switching process  $\beta I[x_t \geq x_c]$ . The conditional mean of the autoregressive process, denoted by,  
 30  $\bar{a} + s_1(t\varepsilon_1)$ , changes slowly. The autocorrelation, denoted by,  $\rho(s_2(t\varepsilon_2))$ , also changes slowly.  
 31 The specification (1) is designed to capture the idea that the variance of the state variable  $x_t$   
 32 computed on moving windows on the fast time scale could be used as an early warning indicator  
 33 of  $|\rho(s_2(t\varepsilon_2))|$  passing through 1 from below on the slow time scale for the pure autoregressive  
 34 case where the switching parameter  $\beta = 0$ . The switching parameter is added to capture the idea  
 35 of flickering. Symbol definitions are collected in Table A.1.

36  
 37 In (1), the dynamics of the state variable  $x$  involve the conditional mean  $\bar{a}$ , two slow  
 38 variables  $s_1$  and  $s_2$ , a shock process  $be_{t+1}$ , and a switching process  $\beta I[x_t \geq x_c]$ . We discuss the  
 39 slow variables, shocks and switching processes in turn.  
 40  
 41

42 The slowly-changing variables follow two functions,  $s_1(z), s_2(z)$  which are differentiable  
 43 in  $z$ . They are written as  $s_i(t\varepsilon_i), i = 1, 2$  to emphasize that as  $t$  increases by one step, the quantities  
 44  $s_i(t\varepsilon_i)$  increase by a very small amount since the functions are differentiable and the  
 45  $\varepsilon_i > 0, i = 1, 2$  are a very small positive numbers.

46  
 47 Shocks  $\{e_i\}$  are assumed to be uncorrelated over time and to follow a second order  
 48 stationary sequence of random variables, each with mean zero and variance  $\sigma_e^2$ . In equation (5)  
 49 below, we assume the stochastic processes  $\{e_{1t}\}, \{e_{2t}\}$  are independently and identically  
 50 distributed over time, each with zero mean and unit variance. In an ecological context one might  
 51 think of these shocks as higher dimensional “left-out” dynamics that impinge upon the dynamics  
 52 under scrutiny. In the lake food web example presented in the main text, the shocks represent  
 53 variations in temperature, irradiance, nutrients or some other exogenous variable. More generally  
 54 they correspond to process errors in statistical models of ecosystem dynamics (Hilborn and  
 55 Mangel 1997).

56  
 57 Switching is represented by the indicator function  $1[.]$ . This function is one if the event in  
 58  $[.]$  occurs and is zero otherwise. In connection to the food web example of the main text, note  
 59 that a predator-prey interaction in which  $x_2$  preys on  $x_1$  could be represented by the two  
 60 dimensional version of equation (1), i.e. equation (5) below if the  $\beta_{12}$  and  $b_{12}$  terms in the right  
 61 side of equation (5) were negative so a positive shock or a jump up in  $x_{2t}$  decreases  $x_{1t}$ .  
 62 Returning to the one dimensional case, Fig. 2 of the main text shows an example where the  
 63 switching point or threshold is  $x_c = 2$ . The dynamical law of motion changes discontinuously as  
 64  $x$  passes through the threshold point  $x_c = 2$ .

65  
 66 Switching functions are useful for representing discontinuous shifts in complex systems  
 67 and we will use them extensively in this appendix. Although switching functions are not  
 68 differentiable at the discontinuity, they can be approximated closely by functions that are  
 69 differentiable. Switch terms, which are closely related to sigmoid functions used in many  
 70 ecological models, can be smoothed as follows. Note that as  $q$  tends to infinity the function,  
 71  $g(x, q) := x^q / (x^q + x_0^q)$  tends to an “up” switch at  $x_0$ . The notation ‘:=’ means “is defined to be”.  
 72 That is as  $q \rightarrow \infty$ ,  $g(x, q)$  converges to the following function that we denote as  $g_\infty(x)$ .

73

$$g_\infty(x) = 0, \text{ for } x < x_0,$$

74 (2)  $g_\infty(x) = 1/2, \text{ for } x = x_0,$

$$g_\infty(x) = 1, \text{ for } x > x_0$$

75  
 76 If we slightly modify the definition of the function,  $1[x \geq x_0]$ , to the following,

77

$$1^*[x \geq x_0] = 0, \text{ for } x < x_0$$

$$(3) 1^*[x \geq x_0] = 1/2, \text{ for } x = x_0,$$

$$1^*[x \geq x_0] = 1, \text{ for } x > x_0$$

79

80 then we see that we can approximate a switching function as closely as we wish with a smooth  
81 approximating function.

82

83 Squealing can occur in equation (1) as a slow variable moves the curve upward so that  
84 the lower equilibrium approaches the threshold, or downward so that the upper equilibrium  
85 approaches the threshold. When squealing occurs,  $\rho^2$  approaches one from below which  
86 increases the steady state variance  $\bar{\sigma}^2 = b^2 \text{var}(e_t) / (1 - \rho^2)$ . This point is discussed in detail in  
87 the appendix of Biggs et al. (2009).

88

89 Using this framework we can highlight the distinction between squealing and flickering  
90 by simplifying to a model where squealing cannot occur, but flickering can occur. We will fix  
91 the value of  $\rho$  in equation (1) for all  $t$ , where  $0 < \rho < 1$ . We will bound the shocks so that  $\{e_t\}$  is  
92 a second order stationary stochastic process of uncorrelated binary random variables, each with  
93 mean zero and taking the value -1 with probability  $1/2$  and +1 with probability  $1/2$ . The result is

94

$$(4) x_{t+1} = \bar{a} + \rho x_t + b e_{t+1} + \beta 1[x_t \geq x_c]$$

96

97 We portray this system setting the threshold point  $x_c = 2$  in Fig. 2 of the main text. The system  
98 has two stable equilibria and an unstable equilibrium (Fig. 2A). Squealing cannot occur because  
99 the slope  $\rho$  is constant. However, flickering can occur. Indeed, flickering can occur even if the  
100 slope  $\rho$  is zero (Fig. 2B). For certain values of the parameter  $\bar{a} > 0$  it is possible for the shocks to  
101 move the system between the two positive equilibria. This highlights the contrast between early  
102 warning signs that are based on a slow variable increasing  $\rho^2$  towards one from below which  
103 increases the steady state variance  $\bar{\sigma}^2 = b^2 \text{var}(e_t) / (1 - \rho^2)$  and early warning signals that are  
104 produced by flickering from one attractor to another.

105

106

#### MUFLING AND MAGNIFYING

107

108 This section derives conditions for muffling or magnifying variance when critical  
109 transitions interact. First we will introduce a general model of a two-dimensional switching  
110 system. We then define muffling and magnifying in a precise mathematical way. Finally, we  
111 determine conditions for muffling and magnifying that account for flickering and squealing.  
112 Three cases are considered: the long-run stationary variance, the one-step ahead variance, and  
113 finally the variance for a finite number  $h$  of steps. The last of these is the most difficult to derive  
114 but perhaps the most relevant for analysis of ecological time series.

115

116

117

118

*A Two-Dimensional Switching System*

Throughout this section of the paper, we will consider a two-dimensional switching system that serves as a stark representation of an ecosystem where critical transitions can occur in each of two subsystems. The model is given by

$$(5.a) \quad x_{1,t+1} = \bar{a}_1 + \rho_{11}x_{1t} + \rho_{12}x_{2t} + b_{11}e_{1,t+1} + b_{12}e_{2,t+1} + \beta_{11}I[x_{1t} \geq x_{1c}] + \beta_{12}I[x_{2t} \geq x_{2c}]$$

$$(5.b) \quad x_{2,t+1} = \bar{a}_2 + \rho_{21}x_{1t} + \rho_{22}x_{2t} + b_{21}e_{1,t+1} + b_{22}e_{2,t+1} + \beta_{21}I[x_{1t} \geq x_{1c}] + \beta_{22}I[x_{2t} \geq x_{2c}] + S_2(x_{3t}) - \beta_{23}I[x_{3t} \geq x_{3c}]$$

We will assume that the autoregression parameters  $\rho$  are functions of very slowly-moving variables as in equation (1), but we will not write them as functions in order to simplify notation. We also assume that  $x_{3t}$  operates on a much slower time scale than  $x_{1t}$  and  $x_{2t}$ . Moreover we assume the slow variable  $x_{3t}$  is deterministic since its time scale is much slower than the simultaneous time scales that we are assuming for the dynamics of the other state variables. Here  $\{e_{it}\}, i=1,2$  are second order stationary stochastic processes that are uncorrelated over time and where each has mean zero and unit variance. The  $e_{i,t}$  are shocks to species  $x_1$  and  $x_2$ . The  $b$  parameters are impact factors of these shocks on each species. While our analysis focuses on the case of upward switches (or jumps) in both  $x_{1t}$  and  $x_{2t}$  as well as  $x_{3t}$ , equations (3) are general.

It is useful to write (5a,b) in matrix form

$$(5.c) \quad x_{t+1} = \bar{a} + \rho x_t + b e_{t+1} + \beta I[x_t \geq x_c] + f_t$$

where now  $x_s, \bar{a}, \rho, b, \beta, x_c, e_s, f_t$  are 2x1 column vector, 2x1 column vector, 2x2 matrix, 2x2 matrix, 2x3 matrix, 2x1 column vector, 2x1 column vector, and 2x1 column vector, respectively. Note that the elements of the 2x1 vectors and 2x2 and 2x3 matrices are defined to be compatible with (5.a,b) above.

An important assumption is evident from the considering the very simple case where the 2x3 matrix  $\beta$  is the zero matrix and the forcing term  $f_t$  is zero. We use the suggestive notation  $\sigma = b$  in (6a) and the following below. Then using the lag operator  $L$  we have

$$(6a) \quad x_t = (I - \rho L)^{-1}(\bar{a} + \sigma e_t) = (I - \rho)^{-1}\bar{a} + (I - \rho L)^{-1}\sigma e_t$$

Recall that the lag operator  $L$  is defined by the equation,  $Lx_t = x_{t-1}$ . Note that  $La=a$  for any constant vector  $a$ . The lag operator is a convenient tool for doing calculations with autoregressive processes. For example, see the calculations in equation (6c) below.

We assume that the matrix series

161 (6b)  $I + \rho + \rho^2 + \dots$

162

163 converges in order that the stationary distribution of (6a) exist and be well defined. Hence we  
 164 assume that the norm  $\|\rho\| < 1$  for a matrix norm  $\|\cdot\|$  such that  $\|AB\| \leq (\|A\|)(\|B\|)$  for any two  
 165 matrices A,B. This will ensure that the matrix series in (6b) converges. A commonly used norm  
 166 is  $\|A\|_2 = \max\{|Ax|_2 / |x|_2\}$  where  $|x|_2$  denotes the usual Euclidean norm of the vector x, i.e.

167  $|x|_2 = \left(\sum_{i=1}^n x_i^2\right)^{1/2}.$

168

169 Calculations and concepts below will also consider the dynamics of  $x_{it}$ ,  $i=1,2$  ignoring  
 170 the interactions with the rest of the system.

171

172 (6c)  $x_{it} = (1 - \rho_{ii}L)^{-1}(\bar{a}_i + \sigma_{ii}e_{it}) = (1 - \rho_{ii})^{-1}\bar{a}_i + (1 - \rho_{ii}L)^{-1}\sigma_{ii}e_{it}$ ,  $i=1,2$ .

173

174 We may use (6) to compute h-step-ahead forecast errors as well as the long run variance-  
 175 covariance matrix of the vector x. Linear expressions like (6) are used in constructing early  
 176 warning signals in nonlinear systems via linearizations of nonlinear stochastic dynamical  
 177 systems around deterministic steady states (called “small noise” expansions; Biggs et al. 2009,  
 178 Williams 2004).

179

### 180 *Conditions for Muffling or Magnifying Variance*

181

182 We define muffling and magnifying in terms of the relative magnitudes of two variances:  
 183 the variance of  $x_I$  as if it existed alone, separate from the interacting system, versus the variance  
 184 of  $x_I$  when it is part of the interacting system. If the first variance ( $x_I$  alone) exceeds the second  
 185 variance ( $x_I$  embedded in the whole system), then the system interactions muffle signals from  $x_I$ .  
 186 If the first variance is less than the second variance then the signals are magnified by the full  
 187 system of interactions.

188

189 In this sub-section of the paper, we will restrict analysis to a system that cannot flicker  
 190 (because there are no switches) but it can squeal because of the very slow change in  $\rho$ . That is we  
 191 set  $\beta = 0$ . We use this simplified system to introduce some basic features of muffling and  
 192 magnifying for the stationary long-term variance and the one-step ahead forecast variance. In the  
 193 next subsection, we return to the more general case where  $\beta \neq 0$  and consider the h-step ahead  
 194 forecast errors in a system that can both flicker and squeal.

195

196 First we consider the whole system. We compute the variance-covariance matrix of the  
 197 stationary distribution of the vector  $x_t$  from (6a) to obtain

198

199 (7a)  $E_{\infty}x_t x_t' = \sum_{n=0}^{\infty} \rho^n b \Sigma_e b' \rho^n$

200

201 where  $E_{\infty} x_t x_t'$  denotes the 2x2 variance covariance matrix of  $x$  computed w.r.t. the stationary  
 202 distribution computed from (6a). Here  $\Sigma_e := E e_t e_t'$  the variance-covariance matrix of the  $e_t$  which  
 203 is independent of  $t$  by stationarity. The upper prime on a matrix denotes transpose. Equation (7a)  
 204 is computed using the assumption,  $E e_t e_s' = 0$ , for all  $s, t, s \neq t$ . Recall that we are assuming that  
 205 the stochastic process of 2x1 random shock vectors,  $\{e_t\}$ , are uncorrelated over time although  
 206 they may be contemporaneously correlated. The contemporaneous correlation will play a role in  
 207 muffling and magnifying below.

208  
 209 Second, we use (6c) to compare the variance of the stationary distribution of  $x_1$  alone as  
 210 if it were not part of the 2x2 system and compare that variance with the variance of  $x_1$  taking  
 211 into account the interactions of  $x_1$  with  $x_2$  in the 2x2 system in which  $x_1$  is embedded. The right  
 212 side of the inequality (7b) below is the variance of  $x_1$  alone. It is computed using (6c). The left  
 213 side of the inequality (7b) below is the variance of  $x_1$  taking into account the interaction of  $x_2$   
 214 with  $x_1$ . It is computed using (6a). Define  $\sigma_{x_1, x_1, \infty} := [\sum_{n=0}^{\infty} \rho^n b \Sigma_e b' \rho^n]_{11}$ .

215  
 216 Third, in order to locate sufficient conditions for the interactions with the rest of the  
 217 system to muffle or magnify the variance of  $x_1$ , we locate sufficient conditions such that the  
 218 inequality  
 219

$$220 \quad \begin{aligned} \text{muffle } \sigma_{x_1, x_1, \infty} &:= [\sum_{n=0}^{\infty} \rho^n b \Sigma_e b' \rho^n]_{11} < b_{11}^2 \Sigma_{e11} / (1 - \rho_{11}^2) \\ \text{magnify } \sigma_{x_1, x_1, \infty} &:= [\sum_{n=0}^{\infty} \rho^n b \Sigma_e b' \rho^n]_{11} > b_{11}^2 \Sigma_{e11} / (1 - \rho_{11}^2) \end{aligned}$$

221  
 222 holds. Inequality (7b) compares the variance of  $x_1$  taking into account interactions with the rest  
 223 of the 2x2 system with the stand-alone variance computed using (6c). We explain the notation in  
 224 (7). First, for any matrix  $A$ ,  $[A]_{ij}$  denotes the  $(i,j)$ 'th element of the matrix  $A$ . Second,  $\sigma_{x_1, x_1, \infty}$   
 225 denotes the variance of  $x_1$  computed at the stationary distribution, i.e.  $\sigma_{x_1, x_1, \infty}$  is the  $(1,1)$  element  
 226 of the 2x2 matrix in (7a). At the risk of repeating, we assumed  $E e_m e_n' = 0, m \neq n, E e_n e_n' = \Sigma_e$  to  
 227 compute (7a). To put it another way, recall that we assume the vector valued second order  
 228 stationary stochastic process  $\{e_t\}$  is serially uncorrelated over time with mean vector equal to the  
 229 zero vector. The variance covariance matrix  $\Sigma_e$  is constant by second order stationarity. As noted  
 230 above we need to assume that the norm  $\|\rho\| < 1$  for a matrix norm  $\|\cdot\|$  such that  
 231  $\|AB\| \leq (\|A\|)(\|B\|)$  for any two matrices  $A, B$  so that the series in (7) converges.

232  
 233 There is an equivalent expression for (7a) which is useful for reducing the location of  
 234 sufficient conditions for (7b) to a manageable task. Using (6) we compute  
 235

$$(7c) \quad E_{\infty} x_t x_t' = \rho E_{\infty} x_t x_t' \rho' + b \Sigma_e b'$$

237  
238 On the surface it does not look like (7c) is helpful since it is a matrix fixed point equation. But  
239 symmetry of the moment matrix  $M := E_{\infty} x_t x_t'$  implies (7c) is just a system of three equations in  
240 three unknowns,  $M_{11}, M_{12} = M_{21}, M_{22}$ . Hence the system (7c) may be expressed as a linear  
241 system of three equations and three unknowns. This system can be solved using Cramer's Rule.  
242 We will use this method below to locate sufficient conditions on (7c) for muffling and  
243 magnifying where these concepts are introduced in the definition below.

244  
245 Definition 1 (Long Run Signal Muffling (Magnifying)): We say that the long run signal on  $x_1$  is  
246 *muffled (magnified)* if the muffling part of (7b) (the magnifying part of (7b)) holds. A similar  
247 definition holds for  $x_2$ .

248  
249 The meaning of "muffled" and "magnified" is intuitive. On the one hand, if the  $x_1$ -part of the  
250 system were independent of the rest of the system except for a variable that pushed the  $x_1$ -  
251 dynamics towards a local bifurcation then the early warning signal would be increasing  $x_1$ -  
252 variance as the local bifurcation is approached because the absolute value of the slope of the  $x_1$ -  
253 linearization is approaching one. That local  $x_1$ -variance is the right side of inequality (7b). On  
254 the other hand, the left side of inequality (7b) is the local variance of  $x_1$  taking into account the  
255 interactions with the rest of the system when  $x_1$  is not independent of the rest of the system.

256  
257 Definition 2 (1-step-ahead-forecast error muffling (magnifying)): We say that the 1-step-ahead  
258 forecast error is *muffled* if

$$(8a) \quad [b \Sigma_e b']_{11} < b_{11}^2 \Sigma_{e,11},$$

261  
262 And we say that the 1-step-ahead forecast error is *magnified* if

$$(8b) \quad [b \Sigma_e b']_{11} > b_{11}^2 \Sigma_{e,11}.$$

265  
266 A bit of matrix algebra shows that (8) holds iff

$$(9a) \quad |b_{12}| < 2b_{11} |\Sigma_{12,e}| / \Sigma_{22,e}$$

$$(9b) \quad |b_{12}| > 2b_{11} |\Sigma_{12,e}| / \Sigma_{22,e}$$

271  
272 For example, the "<" part of inequality (9) holds when the shocks to  $x_1$  and  $x_2$  have a large  
273 enough absolute value of correlation and the standard deviation of the shock to  $x_1$  is large  
274 enough relative to the direct impact of a shock to  $x_2$  to  $x_1$ .

275

276 We are now ready to consider the case of h-step ahead forecast errors. We may compute  
 277 these objects using (6a). We obtain for the h-step-ahead forecast error vector,  
 278

$$279 \quad (10) \quad x_{t+h} - x_{t+h|t} = be_{t+h} + \rho be_{t+h-1} + \rho^2 be_{t+h-2} + \dots + \rho^{h-1} be_{t+h-(h-1)}$$

280  
 281 The variance covariance matrix is given by  
 282

$$283 \quad (11) \quad E\{(x_{t+h} - x_{t+h|t})(x_{t+h} - x_{t+h|t})'\} = b\Sigma_e b' + \rho b\Sigma_e b' \rho' + \dots + \rho^{h-1} b\Sigma_e b' \rho'^{h-1}$$

284  
 285 Note that (11) converges to (7a) as h tends to infinity provided that  $\|\rho\| < 1$ .  
 286

287 Expression (11) exposes two interesting points. First, if the 2x2 matrix  $\rho$  is diagonal the  
 288 condition for muffling of h-step-ahead forecast variance is the same as for one-step ahead  
 289 forecast variance, i.e. expression (8). This is so because the  $\rho$ -specific terms cancel off both  
 290 sides of the inequality. This will not hold for the general case where  $\rho$  is not a diagonal matrix.  
 291 Second, as  $\|\rho\|$  approaches one from below, the right side of expression (11) will tend to  
 292 become larger and the right side of equation (11) will tend to become infinite as h tends to  
 293 infinity. This latter statement is made rigorous in the Appendix to Biggs et al. (2009).  
 294

#### 295 *Variance of h-step Ahead Forecast Errors With Flickering and Squealing*

296  
 297 We now have the background material needed for the case that is perhaps most useful for  
 298 analyzing real-world ecosystems – finite-horizon h-step ahead forecast errors where both  
 299 flickering and squealing are possible. We now assume that the the 2x2 matrix  $\beta$  is nonzero in  
 300 (12) below. Switches and therefore flickering are possible. To compute h-step-ahead forecast  
 301 errors, analysis must therefore take into account the possibility of switches between attractors.  
 302

303 Let us assume that the forcing term  $f_t = 0$ , for all t in order to break the analysis down  
 304 into manageable units. We begin by looking at conditions for muffling due to offsetting jumps  
 305 (or drops) to occur for 2-step-ahead forecast errors. This extra effect can not occur for 1-step-  
 306 ahead forecast errors since  $x_{t+1} - x_{t+1|t} = be_{t+1}$ , i.e. we need at least two periods to pick up the  
 307 effect of jumps. Compute, using (3.c), to obtain  
 308

$$309 \quad (12) \quad fe_{t+2} := x_{t+2} - x_{t+2|t} = be_{t+2} + \rho be_{t+1} + \beta(I[x_{t+1} \geq x_c] - I[x_{t+1} \geq x_c]_t)$$

310  
 311 where  
 312

$$313 \quad (13) \quad I[x_{t+1} \geq x_c]_t := E\{I[x_{t+1} \geq x_c] | x_t\}.$$

314  
 315 We compute  
 316

$$317 \quad (14) \quad E_t\{fe_{t+2} fe_{t+2}'\} = b\Sigma_e b' + \rho b\Sigma_e b' \rho' + \rho b(E_t e_{t+1} z_{t+1}') \beta' + \beta(E_t z_{t+1} e_{t+1}') b' \rho' + \beta(E_t z_{t+1} z_{t+1}') \beta'$$

318

319 where  $E_t\{\cdot\} := E\{\cdot\} | x_t$  and  $z_{t+1} := (I[x_{t+1} \geq x_c] - I[x_{t+1} \geq x_c]_t)$ . We see right away that the first,  
 320 second, and last terms of (14) are positive (in the matrix sense of being positive definite  
 321 matrices). Therefore they can only magnify the signal. However, terms three and four could be  
 322 positive or negative. If they are negative and sufficiently large, they could cause muffling of the  
 323 signal.

324  
 325 Equation (14) is crucial for understanding h-step-ahead variance. Because it is a  
 326 complicated expression, we will exposit it by the following steps. First we study (14) for the  
 327 scalar case. This task is carried out in equations (15)-(20) below. Second, we study (14) for a two  
 328 variable case where the feedback from  $x_2$  to  $x_1$  is zero, i.e.  $\rho_{21} = 0 = \beta_{21}$ , i.e. the  $\rho$  matrix is  
 329 triangular. Equation (21) describes this system. This case is motivated by the trophic cascade  
 330 example which is analyzed in the main text. Even with this simplification, it is useful to begin by  
 331 assuming the matrix  $\rho = 0$  in order to focus on flickering by excluding squealing. This task is  
 332 carried out in equations (22)-(27) below. In the case of h-step-ahead forecast errors the strength  
 333 of squealing as the leading eigenvalue of the matrix  $\rho$  approaches one is very limited for small  
 334 h. This signal, in contrast to flickering, only becomes strong for large h. Hence we will study the  
 335 case of nonzero  $\rho$  only for the case  $h = \infty$ . This case is studied in equations (28)-(31) below.

336  
 337 We compute (14) for the scalar case. Since we are interested in warning signals of a  
 338 critical transition, we compute (14) under the assumption that  $x_{t-1} < x_c$ , i.e. no critical transition  
 339 has yet occurred. We first focus on the case where  $x_c$  is crossed from below due to gradual  
 340 increase in a slow driving variable, which we call an ‘‘upcrossing.’’ Then we discuss the case  
 341 where  $x_c$  is crossed from above, which we call a ‘‘downcrossing’’.

342  
 343 We obtain, for both cases of upcrossing and downcrossing,  
 344

$$345 \quad (15) \quad E_t\{fe_{t+2}^2\} = b^2\sigma_e^2 + \rho^2b^2\sigma_e^2 + 2\rho b\beta(E_t e_{t+1} z_{t+1}) + \beta^2(E_t z_{t+1}^2)$$

346  
 347 where we now compute each of the last two individual terms under the assumption that no  
 348 critical transition has yet occurred and for an upcrossing. We compute,  
 349

$$350 \quad (16) \quad \begin{aligned} & I[x_{t+1} \geq x_c]_t := E\{I[x_{t+1} \geq x_c] | x_t\} \\ & = E\{I[\bar{a} + \rho x_t + b e_{t+1} \geq x_c] | x_t\} \quad , \\ & = 1 - F_e((x_c - \bar{a} - \rho x_t) / b) \end{aligned}$$

351  
 352 where  $F_e(w) := \Pr\{e_{t+1} \leq w\}$  is the cumulative distribution function of the shock and is  
 353 independent of t by stationarity. We compute the conditional covariance variance of z with the  
 354 shock and the conditional variance of z. We obtain  
 355

$$\begin{aligned}
& E_t e_{t+1} z_{t+1} \\
356 \quad (17) &= E_t \{e_{t+1} (\mathbb{1}[x_{t+1} \geq x_c] - \mathbb{1}[x_{t+1} \geq x_c]_t)\} \\
&= \int_{e \geq (x_c - \bar{a} - \rho x_t)/b} e dF_e > 0
\end{aligned}$$

357

358 where the positive right side of (17) follows from  $\int_e e dF_e = 0$  and the fact that the right side is

359 integrating over larger values of  $e$ ,

360

$$\begin{aligned}
361 \quad (18) \quad E_t z_{t+1}^2 &= E_t [(\mathbb{1}[x_{t+1} \geq x_c] - \mathbb{1}[x_{t+1} \geq x_c]_t)]^2 \\
&= \{E_t[\mathbb{1}[x_{t+1} \geq x_c]]\} \{(1 - E_t[\mathbb{1}[x_{t+1} \geq x_c]_t])\}
\end{aligned}$$

362

363 Using (16) to compute the terms in  $\{.\}$  in (18) we obtain

364

$$365 \quad (19) \quad E_t z_{t+1}^2 = (F_e((x_c - \bar{a} - \rho x_t)/b))(1 - F_e((x_c - \bar{a} - \rho x_t)/b)).$$

366

367 We collect our computations and end up with a full expression for the right side of equation (15).

368

$$\begin{aligned}
369 \quad (20a) \quad E_t \{f e_{t+2}^2\} &= b^2 \sigma_e^2 + \rho^2 b^2 \sigma_e^2 + 2\rho b \beta \left( \int_{e \geq (x_c - \bar{a} - \rho x_t)/b} e dF_e \right) \\
&+ \beta^2 (F_e((x_c - \bar{a} - \rho x_t)/b))(1 - F_e((x_c - \bar{a} - \rho x_t)/b))
\end{aligned}$$

370

371 Formula (20a) shows a contrast between the potential power of an early warning signal  
372 based upon  $\rho$  slowly increasing (squealing) in contrast to an early warning signal based upon  
373  $x_{t+1}$  passing through a critical transition where there is a jump (flickering). Note that, in the case  
374 where the product of the autoregression parameter  $\rho$ , shock impact  $b$ , and switch magnitude  $\beta$  is  
375 non-negative ( $\rho b \beta \geq 0$ ) the covariance between the shock and  $z$  does not muffle the signal. Note  
376 also that the jump signal is strongest when  $F_e = 1/2$  because that is when the last term on the  
377 right side of equation (20) is maximum at the value  $\beta^2 / 4$ . That is, the signal is maximum  
378 strength at the median. If the median is zero (a natural median for a mean zero random variable)  
379 then we have the signal is at maximum strength when  $\bar{a} + \rho x_t = x_c$ . Note that when  $\rho = 0$  the  
380 signal is at maximum strength when  $\bar{a} = x_c$ . Hence if there is a slow variable  $S$  that moves  $\bar{a}(S)$   
381 gradually closer to  $\bar{a}_c := x_c$  we see from (20) that the signal from the variance of 2-step-ahead  
382 forecast errors of impending critical transition gets stronger when  $\rho b \beta \geq 0$ . This flickering  
383 signal is independent of any signal based upon increasing variance from the movement of the  
384 autocorrelation coefficient  $\rho$  towards unity from below.

385

386 Now consider the case of a down crossing of  $x_c$  where the value of  $x$  falls by  $\beta$ . We  
387 obtain, (letting  $e_{\min}$  denote the lower bound of the set of  $e$ 's with positive probability, which may  
388 be  $-\infty$ ),

389

$$(20b) \quad E_t \{ f e_{t+2}^2 \} = b^2 \sigma_e^2 + \rho^2 b^2 \sigma_e^2 + 2\rho b (-\beta) \left( \int_{e_{\min}}^{(x_c - \bar{a} - \rho x_t)/b} -e dF_e \right) \\ + \beta^2 (F_e((x_c - \bar{a} - \rho x_t)/b))(1 - F_e((x_c - \bar{a} - \rho x_t)/b))$$

391

392 Notice that even if  $\rho b \beta \geq 0$  the second to the last term now muffles the signal when a jump is393 negative. This is so because the term,  $\int_{e_{\min}}^{(x_c - \bar{a} - \rho x_t)/b} e dF_e < 0$ . This latter conclusion follows from the

394 mean of “e” being zero and the latter integral being over the lower values of “e”.

395

396

### *Triangular $\rho$ Matrix*

397

398 In trophic cascades, the impact of a top predator to certain prey is stronger than the  
399 impact of these prey on the predator. Such a system can persist if the predator has multiple food  
400 sources as shown in the example of Fig. 1. We represent such a system by a triangular  $\rho$  matrix  
401 and a triangular  $\beta$  matrix in which one feedback is negligible:

402

$$(21.a) \quad x_{1,t+1} = \bar{a}_1 + \rho_{11} x_{1t} + \rho_{12} x_{2t} + b_{11} e_{1,t+1} + b_{12} e_{2,t+1} + \beta_{11} \mathbb{1}[x_{1t} \geq x_{1c}] + \beta_{12} \mathbb{1}[x_{2t} \geq x_{2c}]$$

404

$$(21.b) \quad x_{2,t+1} = \bar{a}_2 + \rho_{22} x_{2t} + b_{22} e_{2,t+1} + \beta_{22} \mathbb{1}[x_{2t} \geq x_{2c}] + f_{2t}$$

406

$$(21.c) \quad f_{2t} := S_2(x_{3t}) - \beta_{23} \mathbb{1}[x_{3t} \geq x_{3c}]$$

408

409 In this system the feedback from  $x_{1t}$  to  $x_{2t}$  is so weak that we approximate it by zero. We shall  
410 start analysis by restricting ourselves to upcrossings and to a situation where no upcrossings have  
411 yet occurred. Notice also that a drop can occur in the  $f_{2t}$  term in (21.b) due, perhaps to a jump in  
412 the biomass of the predator that feeds on  $x_2$ .

413

414

### *Zero $\rho$ Matrix: An Informative Special Case*

415

416 Recall that (14) exhibits a decomposition of forces for muffling (magnifying) into three  
417 components: (i) shocks (through the term  $b \Sigma_e b'$ ), (ii) dynamics (propagated through the matrix  
418  $\rho$ ), and (iii) jumps and drops (captured in the term,  $\beta(E_t z_{t+1} z'_{t+1}) \beta'$ ). The complexity of (14)  
419 reflects the interactions amongst these three forces. In this subsection we obtain useful analytical  
420 results by simplifying the analysis of equation (14) by assuming the matrix  $\rho = 0$  so we can  
421 evaluate muffling or magnifying in a system subject to flickering but not squealing. It makes  
422 sense to focus on the case  $\rho = 0$  for smaller h's, e.g. h=2, because the strength of the squealing  
423 signal, i.e. the increase in variance as the leading eigenvalue of the matrix  $\rho$  approaches one, is  
424 muted unless h is quite large. We have, from (14), for the case where the matrix  $\rho = 0$  and the  
425 forcing term for the dynamics of  $x_{2t}$ , i.e.,  $f_{3t} = 0$ ,

426

$$427 \quad (22) \quad E_t \{ f e_{t+2} f e'_{t+2} \} = b \Sigma_e b' + \beta (E_t z_{t+1} z'_{t+1}) \beta'$$

428

429 We wish to locate sufficient conditions for muffling or magnifying to occur in (22), i.e.,

430

$$431 \quad (23a) \quad (\text{muffling}) \quad [b \Sigma_e b']_{11} + [\beta (E_t z_{t+1} z'_{t+1}) \beta']_{11} < b_{11}^2 \Sigma_{e11} + \beta_{11}^2 [(E_t z_{t+1} z'_{t+1})]_{11}$$

432

$$433 \quad (23b) \quad (\text{magnifying}) \quad [b \Sigma_e b']_{11} + [\beta (E_t z_{t+1} z'_{t+1}) \beta']_{11} > b_{11}^2 \Sigma_{e11} + \beta_{11}^2 [(E_t z_{t+1} z'_{t+1})]_{11}$$

434

435 It is convenient for the computations below to put  $n_{i,t+1} := b_{i1} e_{1,t+1} + b_{i2} e_{2,t+1}$ ,  $i=1,2$ . Note that

436  $\Sigma_n := E n n' = b \Sigma_e b'$  are independent of date  $t$  by stationarity. Using this notation for the shocks,

437

438

$$439 \quad (24) \quad \begin{aligned} & \mathbb{1}[x_{i,t+1} \geq x_{ic}] = \mathbb{1}[\bar{a}_i + n_{i,t+1} \geq x_{ic}], \quad i=1,2 \\ & \mathbb{1}[x_{i,t+1} \geq x_{ic}]_t = 1 - F_{n_i}(x_{ic} - \bar{a}_i), \quad i=1,2 \end{aligned}$$

440

441 We now compute the elements of  $(E_t z_{t+1} z'_{t+1})$ , where  $F_{n_i}, i=1,2$  denotes the cumulative

442 distribution functions of the shocks. Shorten the notation by putting  $E_t z_{t+1} z'_{t+1} := \Sigma_z$  which is

443 independent of date  $t$  by stationarity. We obtain, by computation,

444

$$445 \quad (25) \quad \begin{aligned} & \Sigma_{z,ii} = (1 - F_{n_i}(x_{ic} - \bar{a}_i)) F_{n_i}(x_{ic} - \bar{a}_i), \\ & \Sigma_{z,12} = \Pr\{n_{1,t+1} \geq x_{1c} - \bar{a}_1, \\ & \quad \text{and } n_{2,t+1} \geq x_{2c} - \bar{a}_2\} - \Pi_{i=1}^2 (1 - F_{n_i}(x_{ic} - \bar{a}_i)) \end{aligned}$$

446

447 Of course when the  $n$ 's are independent  $\Sigma_{z,12} = 0$ .

448

449 We have already investigated sufficient conditions for

450 *muffling*,  $[b \Sigma_e b']_{11} < b_{11}^2 \Sigma_{e11}$ , and, *magnifying*,  $[b \Sigma_e b']_{11} > b_{11}^2 \Sigma_{e11}$  in material surrounding

451 equation (8). We turn here to investigating sufficient conditions for muffling and magnifying in a

452 slightly more complicated case,

453

$$454 \quad (26) \quad \begin{aligned} & \text{muffling, } [\beta (E_t z_{t+1} z'_{t+1}) \beta']_{11} < \beta_{11}^2 [(E_t z_{t+1} z'_{t+1})]_{11} \\ & \text{magnifying, } [\beta (E_t z_{t+1} z'_{t+1}) \beta']_{11} > \beta_{11}^2 [(E_t z_{t+1} z'_{t+1})]_{11} \end{aligned}$$

455

456 Straightforward computation, yields the conclusion that (26) holds if and only if,

457

$$458 \quad (27) \quad \begin{aligned} & \beta_{11}^2 \Sigma_{z,11} + 2\beta_{12}\beta_{11}\Sigma_{z,12} + \beta_{12}^2 \Sigma_{z,22} < \beta_{11}^2 \Sigma_{z,11} \\ & \beta_{11}^2 \Sigma_{z,11} + 2\beta_{12}\beta_{11}\Sigma_{z,12} + \beta_{12}^2 \Sigma_{z,22} > \beta_{11}^2 \Sigma_{z,11} \end{aligned}$$

459

460 In the main text we use simulation to investigate cases where  $r_{12}$  is negative, zero or  
 461 positive, where  $r_{12} := \Sigma_{n,12} / (\Sigma_{n,11}^{1/2} \Sigma_{n,22}^{1/2})$  is the correlation coefficient. Since zero correlation is not  
 462 the same as independence we proxy  $r_{12} = 0$  with independence which implies  $\Sigma_{z,12} = 0$  (which is  
 463 not implied by zero correlation because of the nonlinearity of the indicator function). We note  
 464 that for  $\Sigma_{z,12} = 0$ , expression (27) shows that the signal is always magnified by the possibility of  
 465 jumps (drops) over and beyond magnification (muffling) induced by dependence in the shocks.  
 466 Since  $x_2$  preys on  $x_1$  in the example below, the “natural” case is  $\beta_{12} < 0$ . We then have two  
 467 subcases,  $\Sigma_{n,12} < 0$ ,  $\Sigma_{n,12} > 0$ . For the case  $\beta_{12} < 0$ ,  $\Sigma_{n,12} < 0$ , (27) shows that the signal is always  
 468 magnified. This outcome may apply to predator-prey systems because the  $n$  vectors are likely to  
 469 be negatively correlated.

### 470 *Nonzero Triangular $\rho$ Matrix*

471  
 472  
 473 We return now to the case where the 2x2 matrix  $\rho$  is not the 2x2 zero matrix. We assume  
 474 that  $\rho$  is a function of variables that change very slowly, so that squealing and flickering can both  
 475 occur. We shall assume that the matrix norm of  $\rho$  is less than one as well as other regularity  
 476 conditions, e.g. the variance matrices  $\Sigma_e, \Sigma_f$  are finite, so the steady state distribution of  $x_t$   
 477 exists.

478  
 479 We compute the steady state variance covariance matrix of equation (5.c) under the  
 480 assumption that  $\{e_{t+1}\}$  is an Independent and Identically Distributed process across time with  
 481 mean vector zero and finite variance matrix,  $\Sigma_e$ . First we observe that the steady state mean  
 482 vector for  $x$  is given by

$$483 \quad (28) \quad \bar{x} = \bar{a} + \rho \bar{x} + \beta E_\infty l[x_t \geq x_c] + E_\infty f_t := \bar{a} + \rho \bar{x} + \beta \bar{1} + \bar{f}$$

484 where we have shortened the notation by putting  $\bar{1} = E_\infty l[x_t \geq x_c]$  and  $\bar{f} = E_\infty f_t$

485 Let  $y = x - \bar{x}$ . Then

$$486 \quad (29) \quad E_\infty yy' = \rho(E_\infty yy')\rho' + b\Sigma_e b' + R_\infty$$

487 where the notation (“R” for “residual”),  $R_{1,\infty}, R_{2,\infty}$  denote the matrices containing the other terms.  
 488 Recall that muffling or magnifying of variable  $x_i, i = 1, 2$  occurs when

$$489 \quad (30) \quad \begin{aligned} \text{muffling} \quad E_\infty y_i^2 &= \rho_{ii}^2 E_\infty y_i^2 + b_{ii}^2 \Sigma_{e,ii} + R_{1,ii,\infty} < [E_\infty yy']_{ii} = [\rho(E_\infty yy')\rho']_{ii} + [b\Sigma_e b']_{ii} + [R_{1,\infty}]_{ii} \\ \text{magnifying} \quad E_\infty y_i^2 &= \rho_{ii}^2 E_\infty y_i^2 + b_{ii}^2 \Sigma_{e,ii} + R_{1,ii,\infty} > [E_\infty yy']_{ii} = [\rho(E_\infty yy')\rho']_{ii} + [b\Sigma_e b']_{ii} + [R_{1,\infty}]_{ii} \end{aligned}$$

490 where

$$491 \quad (31) \quad R_{1,\infty} = E_\infty (f_t - \bar{f})(f_t - \bar{f})' + \beta E_\infty \{(l[x_t \geq x_c] - \bar{1})(l[x_t \geq x_c] - \bar{1})'\} \beta' + R_{2,\infty}$$

499  
 500 Equation (30) compares the steady state variance of each  $x_i$  when all connections with the rest of  
 501 the system are set equal to zero with the steady state variance of each  $x_i$  when the connections  
 502 are taken into account. A lot of complexity is embedded in the notation of expression (30). We  
 503 observe that muffling (magnifying) comes from three sources: (i) interactions from the  
 504 nondiagonal terms of the  $\rho$  matrix, (ii) interactions from the nondiagonal terms of the  $b$  and  $\Sigma_e$   
 505 matrices, (iii) interactions from the nondiagonal terms of the  $R_{1,\infty}$  matrix. The  $R_{1,\infty}$  matrix is  
 506 complicated because it captures the variance matrices of  $f_t - \bar{f}$ ,  $\mathbb{1}[x_t \geq x_c] - \bar{1}$  as well as the  
 507 cross interactions among the terms,  $f_t - \bar{f}$ ,  $\mathbb{1}[x_t \geq x_c] - \bar{1}$ ,  $y_t - \bar{y}$  all computed at the steady state  
 508 distribution.

509  
 510 We observe from (30) that if all matrices in (28) are diagonal and  $\Sigma_e$  is diagonal, then  
 511 (30) collapses to two independent scalar systems and no issues of muffling (magnifying) can  
 512 arise. Second, we observe that if  $\rho_{ii}^2$  approaches one from below, we should expect the steady  
 513 state variance of  $x_i$  to become infinite. Third, when we consider the variance matrices of  
 514  $f_t - \bar{f}$ , and,  $\mathbb{1}[x_t \geq x_c] - \bar{1}$ , we see that muffling (magnifying) is impacted by interactions within  
 515 the vector of outside forcings as well as interactions within the vector of potential jumps (drops).  
 516 The vector of outside forcings of the dynamics between  $x_1$  and  $x_2$  is due to forces like fish  
 517 predation, habitat modification, etc. Fourth, muffling (magnifying) is also impacted by the cross  
 518 terms in the matrix  $R_{2,\infty}$  in equation (31). Summing up, we see that muffling (magnifying) can  
 519 occur due to (i) interactions in squealing (due to non zero cross terms in the  $\rho$  matrix), (ii)  
 520 interactions in flickering (due to nonzero cross terms in the  $\beta$  matrix and the  
 521  $E_\infty \{(\mathbb{1}[x_t \geq x_c] - \bar{1})(\mathbb{1}[x_t \geq x_c] - \bar{1})'\}$  matrix), (iii) interactions in outside forcing (due to nonzero  
 522 cross terms in the  $E_\infty \{(f_t - \bar{f})(f_t - \bar{f})'\}$  matrix), (iv) interactions in the shocks (due to nonzero  
 523 cross terms in the  $b$  matrix and the  $\Sigma_e$  matrix), (v) interactions in cross product terms (due to  
 524 nonzero cross terms in the  $R_{2,\infty}$  matrix). In view of this complexity, it is difficult to say more  
 525 using analytical methods.

#### 526 LITERATURE CITED

- 527  
 528  
 529 Biggs, R., S.R. Carpenter and W.A. Brock. 2009. Turning back from the brink: Detecting an  
 530 impending regime shift in time to avert it. *Proceedings of the National Academy of Sciences*  
 531 106: 826-831.  
 532  
 533 Hilborn, R. and M. Mangel. 1997. *The Ecological Detective: Confronting Models with Data*.  
 534 Princeton University Press, Princeton, N.J.  
 535  
 536 Williams, N. 2004. Small noise asymptotics for a stochastic growth model. *Journal of Economic*  
 537 *Theory* 119(2):271-298.

538 Table A.1. Symbols used in the mathematical analysis in this paper. Symbols used in the  
 539 simulations are presented in Table 2.  
 540

Symbol	Definition
$1[\cdot]$	Indicator function which is 1 if the event $[\cdot]$ occurs and zero otherwise
$\bar{a}$	conditional mean
$b$	effect of a shock
$E$	expectation operator
$e$	random variable, where $\{e_t\}$ is a stationary sequence of random variables, each with mean zero and variance $\sigma_e^2$
$F_e(w)$	cumulative probability distribution of shocks, i.e. $F_e(w) := \Pr\{e_{t+1} \leq w\}$
$f_t$	exogenous forcing of a system
$g(x, q)$	sigmoid function of $x$ with exponent $q$ ; $g(x, q) := x^q / (x^q + x_0^q)$
$L$	lag operator
$n$	shock effect; $n_{i,t+1} := b_{i1}e_{1,t+1} + b_{i2}e_{2,t+1}$ , $i=1,2$
$Q$	matrix of shocks multiplied by their effects; $Q := b\Sigma_\infty b'$
$q$	exponent of a sigmoid function
$R$	residual matrices used to analyze the case of h-step-ahead forecast errors when the autoregression matrix is nonzero and triangular. The $R$ matrix is complicated because it contains the variance of forcing and switching, and all their cross-interactions, all computed at the steady-state distribution.
$s$	a slowly-changing variable or function
$t$	time
$x$	state variable
$x_c$	critical transition point (threshold) for a state variable
$z$	change in a switching variable over one time step, i.e. $z_{t+1} := (1[x_{t+1} \geq x_c] - 1[x_t \geq x_c])$
$\beta$	jump or drop factor in a switching equation
$\varepsilon$	tiny positive number
$\rho$	autoregression coefficient
$\sigma$	standard deviation
$\Sigma_e$	variance-covariance matrix of shocks, $E(e_t e_t')$

541  
 542  
 543